A STUDY OF THE STRUCTURE AND DISTRIBUTION OF THE NEXUS

M. M. DEWEY, Ph.D., and L. BARR, Ph.D.
With the Technical Assistance of J. TERNAK

From the Departments of Anatomy and Physiology, The University of Michigan, Ann Arbor

ABSTRACT

Nexuses, that is, fusions of plasma membranes of adjacent cells, are described in mammalian smooth and cardiac muscle, median giant axon of earthworm, frog skin, and rat submandibular gland. In smooth muscle they usually occur where a process from one cell either meets a process of, or projects into a neighboring cell. On the other hand, in mammalian heart muscle and in earthworm giant axon the nexuses occur along the intercalated disc and intercellular segmental septa, respectively. Their occurrence between these excitable cells is correlated with propagation of action potentials by an electrical rather than chemical mechanism. Since the nexuses may offer pathways for electric current between cell interiors, it seems possible that they constitute a link in the structural basis for electrical transmission in these systems. In epithelia, nexuses usually appear as part of a terminal bar complex. This is true in the rat salivary gland studied here. In the epidermis of frog skin, nexuses are less numerous between the basilar columnar cells than between the subjacent squamous cells. The nexuses which occur in epithelia in frog skin and rat salivary gland are distributed as though to provide seals against electrochemical backleaks and sites of chemical exchange between cell interiors.

In an earlier report (1) regions of fusion of plasma membranes of adjacent smooth muscle cells were described. The structure at the region of fusion was termed a *nexus*. Attention was called to the probable functional importance of this structure as a site of electrotonic coupling between cells (1, 2). In epithelia, the fusion of adjacent cell membranes at the nexus apparently subserves an additional function: that is, to seal the cells to each other thereby preventing electrochemical backleaks. A number of papers on cardiac muscle (3, 4), neural tissue (5–8), smooth muscle (9–12), and epithelia (13–18) have appeared in which similar structures have been described. Moreover, several terms besides nexus (external compound membrane, (19); quintuple-layered cell interconnection, (13); tight junction, (20); *zonula occludens*, *macula occludens*, (18) have been applied to what is apparently the same structure.

In contrast to the above reports, some investigators do not find the coincidence of the nexus and electrotonic coupling between cells. Several studies on smooth muscle (21–23), septate junctions of giant fibers of earthworm (24), and septate and lateral-motor synapses of the giant fibers of crayfish (25), as well as glial interconnections in the leech (26), show no fusions of adjacent cell membranes where they might be expected to occur. The lack of morphological correlation in these cases may be due to technical problems in the preservation of the fusion of membranes.

This paper has two purposes: one, to report the results of a survey of the cell-to-cell appositions in several tissues in which the occurrence of the nexus could be reasonably suspected on physio-

logical grounds; and two, to provide a more detailed description of the nexus as an anatomical entity. In the latter regard, close attention must be paid to the differences in the structure due to differences in experimental technique. The group of tissues studied here (mammalian intestinal smooth muscle and cardiac muscle, earthworm median giant axon, frog skin and rat salivary gland epithelia) was selected to demonstrate the expected correlation between structure and function. At the same time, it provides a graded series which illustrates the differences in the structural stability of the nexus and the differences in the appearance of the nexus according to fixation techniques.

MATERIALS AND METHODS

The following tissues were studied: (1) *smooth muscle:* circular layer of dog and cat jejunum, taenia coli of guinea pig; (2) *cardiac muscle:* papillary muscles of guinea pig and cat heart; (3) *nerve cord:* median giant axon of earthworm (*Lumbricus*); and (4) *epithelia:* abdominal skin of frog (*Rana pipiens*) and acinar and ductular epithelium of submandibular gland of the rat (Sprague-Dawley strain).

Preparations

Preparations of smooth muscle from the circular layer of cat and dog jejunum were obtained by snipping out samples and fixing them immediately. Other samples of smooth muscle were obtained by first inserting a glass tube into the lumen of the intestine and then cutting around the tube with a razor blade so as to isolate 1- to 5-cm segments. These were also fixed immediately. A better procedure was to remove a 2- to 10-cm segment of jejunum, invert it, slip it over a glass tube, and dissect the mucosa and submucosa away from the circular muscle layer; the remaining muscular tube was removed, pulled right side out again, slipped over the glass tube, and the serosa and longitudinal muscle layer dissected away from the circular muscle layer. Rings of circular muscle were thus dissected free. They were then either fixed immediately or incubated in Krebs-Henseleit (27) solution at 37°C for 2 hours to recover electrical and mechanical responsiveness before fixation. Some rings were slipped over U-shaped glass tubes before they were incubated so that they were at a constant length during both incubation and fixation. Others were mounted on a Grass Force Transducer so that their isometric tension was recorded during incubation, after stimulation, and during fixation. All preparations showed marked contraction during fixation.

Samples of taenia coli of the guinea pig were dissected from the underlying intestine. Some specimens were incubated in Krebs-Henseleit solution at 37°C at constant length, some were left free, and other specimens were not incubated at all.

Some of the papillary muscles of the right ventricle of cat and guinea pig heart were incubated. However, incubation did not change the appearance of the tissues in electron micrographs.

Submandibular glands of male Sprague-Dawley rats were dissected free, and sliced in fixative into pieces approximately 1 millimeter square.

All mammals were anesthetized with Nembutal.

The nerve cords of earthworm were dissected free using a ventral approach. Some worms were anesthetized with 3 per cent urethane, others with 5 per cent ethanol or 1 per cent MS-222 (Sandoz), and still others not at all. The cords were fixed without prior incubation but were spot-checked for electrical excitability and conduction.

Samples of abdominal skin of frog were removed from decapitated, spinally pithed animals and fixed immediately.

FIGURE 1 Smooth muscle from the circular layer of dog small intestine fixed immediately after extirpation. No regions of intercellular contact are observed between adjacent cells. However, areas of increased cytoplasmic density immediately subjacent to the plasma membrane occur independently along the plasma membrane of one cell or in register with similar areas in adjacent cells (arrows). OsO_4-fixed, Vestopal-embedded; section stained with uranyl acetate. × 13,000.

FIGURE 2 Dog intestinal smooth muscle dissected free and soaked for 2 hours in Krebs-Henseleit solution. Note the good quality of preservation of the tissue relative to Fig. 1. On careful inspection, large fibrils can be observed in the cytoplasm, in contrast to Fig. 1. The submembrane cytoplasmic densities are much lighter and the cells are seen to come much closer together in certain regions. These close appositions of adjacent cells are indicated by arrows. Note that the five most central cells are interconnected by such junctions. OsO_4-fixed, Vestopal-embedded; section stained with uranyl acetate. × 17,000.

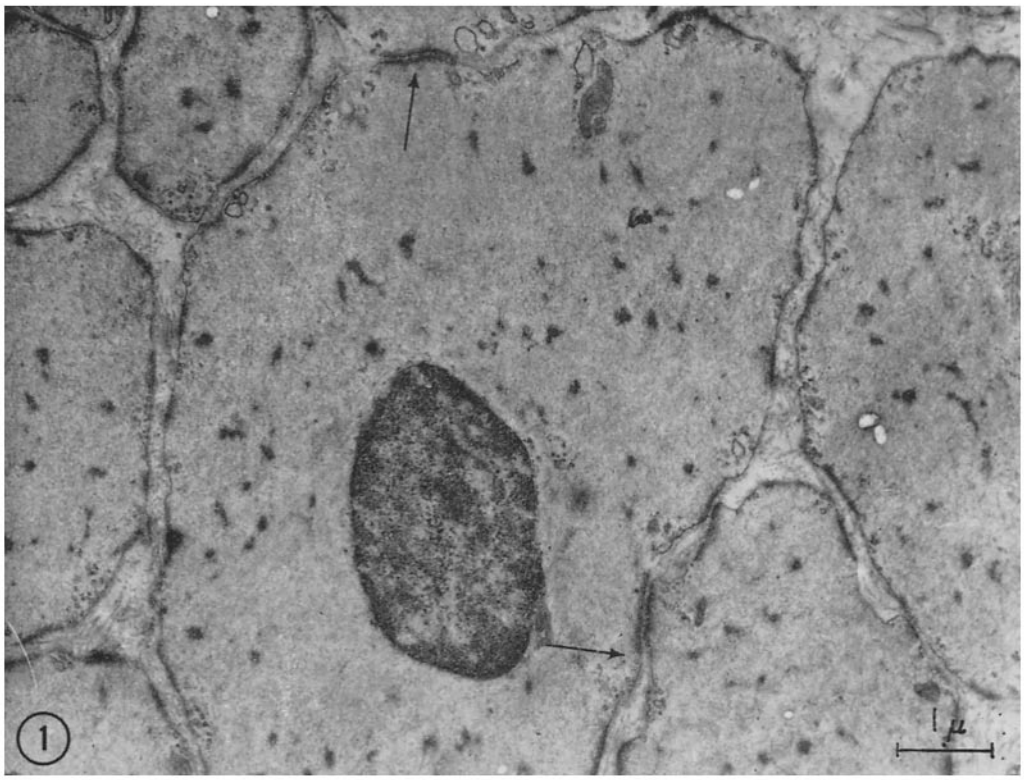
1
1 μ

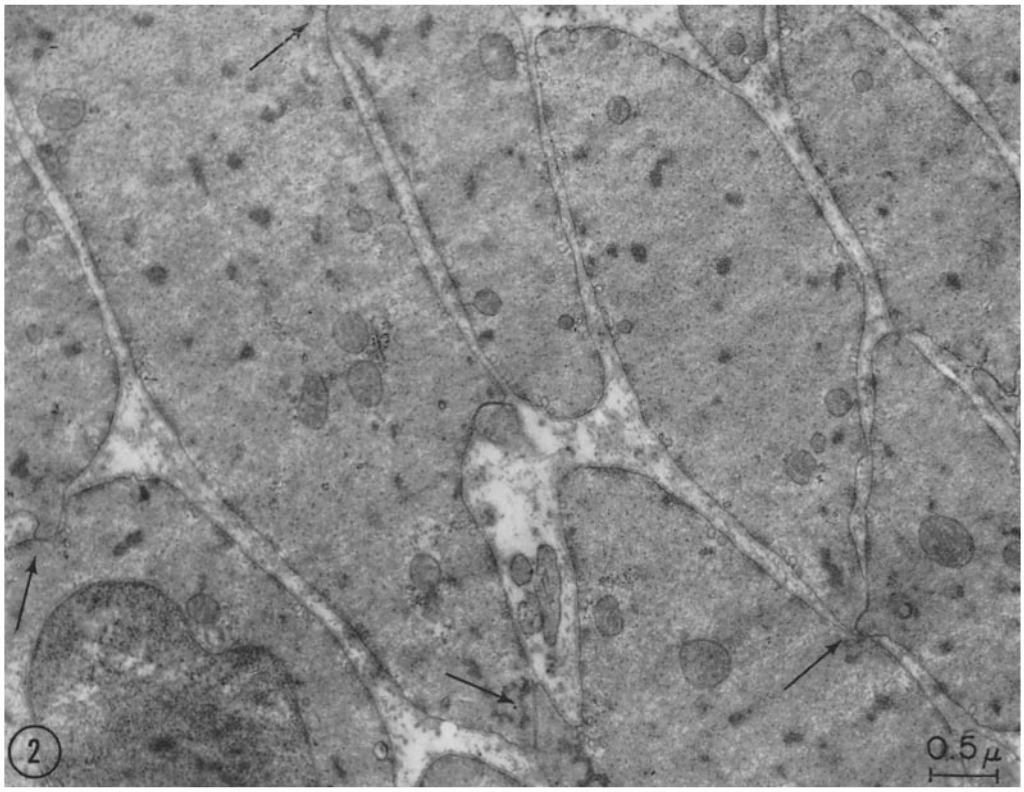
2
0.5 μ

Fixation of Tissues

Osmium tetroxide (OsO_4) fixatives were prepared according to the method of Palade (28), buffered to pH 7.4, and brought to the desired osmolarity by the addition of sucrose. The osmolarity of such fixatives was measured by a Fisk Osmometer and was found to be 344 milliosmolar. Tissues were placed directly into the fixative and fixed for 2 hours at 4°C.

Permanganate fixatives were prepared according to the method described by Luft (29), the final concentration of permanganate being 0.6 or 1.0 per cent. Both potassium and sodium salts were used; however, no difference in the quality of fixation could be noted in the muscles studied. The fixative was at pH 7.4 and was 372 milliosmolar (0.6 per cent) and 420 milliosmolar (1 per cent; Figs. 3 to 6 only). Tissues were placed directly in the fixative for 2 hours at either 4° or 37°C. The lower temperature proved to be more satisfactory. It should be noted that although all fixatives used were slightly hyperosmotic, there was no striking difference in fixation between the 0.6 per cent permanganate and the 1 per cent permanganate.

Processing of Tissues Following Fixation

Tissues were rinsed for 15 to 30 minutes in Krebs-Henseleit or 0.9 per cent NaCl solution and dehydrated in a graded ethanol series, with a 16-hour period in 70 per cent ethanol. They were embedded in either Vestopal W essentially according to the method described by Kurtz (30) or Araldite as described by Luft (31). All embeddings prior to polymerization were subjected to a minimum of 4 hours of vacuum (10 mm Hg).

Sections were obtained on an LKB Ultrotome with diamond knives. They were mounted on grids with supporting films of collodion thinly coated with carbon.

The following methods of staining sections were used: (*a*) Karnovsky's (32) lead method, both A and B procedures, for 10 minutes; (*b*) 1 per cent potassium permanganate according to the method of Lawn (33) for 20 minutes; and (*c*) 2.0 per cent uranyl acetate for 2 to 18 hours (34).

Microscopy

Sections were viewed with RCA EMU 3F and 3G microscopes operating at 50 kv. The latter instrument was used with standard pole pieces and, for portions of the study, with a high-magnification kit coupled with a low-magnification projector pole piece. In all cases, a 25μ objective aperture was employed. Initial magnifications ranging from 3,500 to 53,000 were photographed on Kodak Contrast Lantern Slide Plates.

RESULTS

Smooth Muscle of Dog, Cat, and Guinea Pig

Fixation of muscle pieces immediately upon extirpation from dogs leads to marked contraction of the muscle. No contacts or protoplasmic continuities between smooth muscle cells are apparent, as illustrated in Fig. 1. In fact, each muscle cell is isolated from other muscle cells by connective tissue elements. Dense regions subjacent to the plasma membrane are seen and they are usually in register with similar regions in the adja-

FIGURE 3 Dog intestinal smooth muscle soaked for 2 hours in Krebs-Henseleit solution before fixation. This electron micrograph illustrates nexuses which interconnect three separate smooth muscle cells. Such regions of nexus can involve rather long attenuated cellular processes, as at the arrow. Permanganate-fixed, Vestopal-embedded; section stained with uranyl acetate. × 52,000.

FIGURE 4 An enlargement of the central nexus in Fig. 3. × 230,000.

FIGURE 5 An electron micrograph of a serial section taken deeper in the same tissue as shown in Figs. 3 and 4. Note that while the cellular process (*a*) at the right side of Fig. 3 does not form a nexus, deeper in the tissue as shown in this figure it forms a nexus in the central portion (*b*) of the micrograph. Likewise, the nexus shown in the central portion of Fig. 3 appears to be separating in this figure (upper left) as the plane of section passes to its outer margin. × 70,000.

FIGURE 6 Dog intestinal smooth muscle which has been soaked in Krebs-Henseleit solution for 2 hours prior to fixation. This electron micrograph illustrates another nexus in dog intestinal smooth muscle. Note the uniformity of the thickness of the dark lines. Permanganate-fixed, Vestopal-embedded; section stained with uranyl acetate. × 220,000.

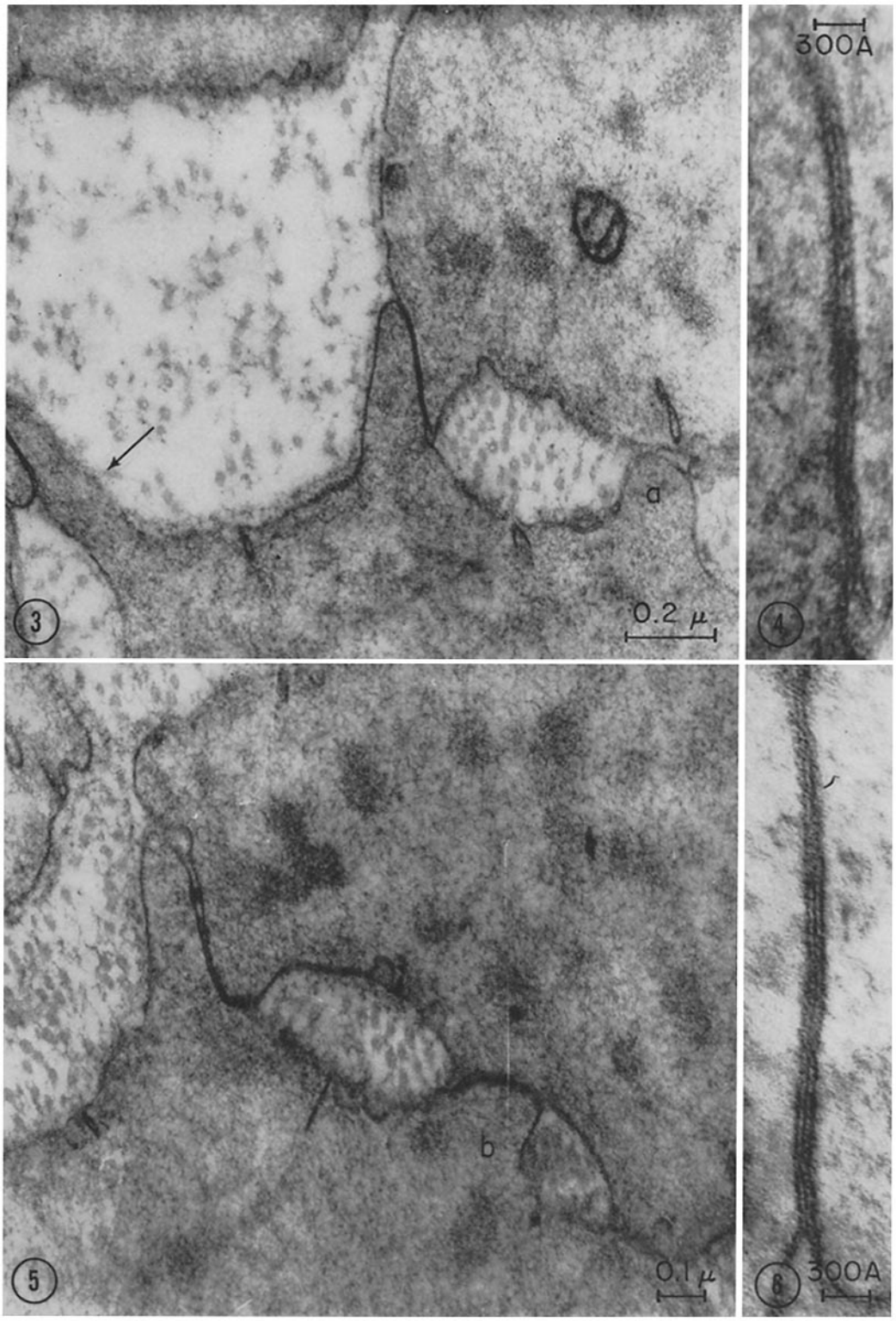
a
0.2 μ
3
300A
4
b
0.1 μ
5
300A
6

cent cells. They may be regions of attachments of myofibrils to the cell membrane (11). These results agree with the observations of other workers (21–23) on various smooth muscles fixed in OsO_4 immediately upon extirpation from the animal (but see reference 12 also).

Since smooth muscle preparations must be incubated in a physiological solution in order to recover electrical and mechanical responsiveness after surgical trauma, the effect of such incubation on the possible anatomical relationship between muscle cells was examined. In OsO_4-fixed, incubated smooth muscle, regions of close apposition between muscle cells are apparent; however, at higher magnifications the osmiophilic components of the adjacent plasma membranes are seen to be 100 A or more apart (Fig. 2). In permanganate-fixed, incubated smooth muscle, however, the adjacent cell membranes appear fused (Figs. 3 to 6). The nexus, as demonstrated here with permanganate fixation, appears as three dark lines of uniform thickness separated by two light lines (Fig. 6). The thickness of the dark lines varies somewhat from preparation to preparation, whereas the over-all thickness of the nexus is remarkably constant (about 140 A; Table I). In any particular instance the nexus is narrower than the two component membranes merely apposed.

Even with permanganate fixation, the nexus between smooth muscle cells is a labile structure under the rigors of preparation and fixation. The nexus was never observed or observed with frequent small regions of separation of the component plasma membranes, except when the tissue was either fixed at a constant length or incubated long enough to recover responsiveness prior to fixation. It is better to do both. Fixation at a fixed-length by perfusion, *in situ*, proved to be as unsatisfactory for the demonstration of nexuses as immediate fixation of small pieces snipped free of the intestine. Thus, the demonstration of nexuses in dog intestinal smooth muscle depended on the proper fixation of physiologically responsive tissue. In a word, the nexus of dog intestinal smooth muscle is labile.

In cat intestinal smooth muscle, however, the nexuses are less labile, more frequent, and involve greater areas. The last is often the result of a projection of one cell into another. These differences can be seen by comparing Figs. 2, 3, and 5 of dog intestinal muscle with Figs. 7, 9, and 10 of cat intestinal muscle. The frequency of nexuses between smooth muscle cells is commensurate with the assumption that the cells of these tissues are, in fact, interconnected.

The geometry of the nexal regions in smooth muscle is of considerable anatomical and physiological interest. The nexal regions observed can be classified roughly into two major types, *i.e.* simple abutment of adjacent cells or projections of one cell into another. The former is more frequent in dog intestinal muscle and the latter in cat and guinea pig intestinal muscle. The simple abutment type of nexus often appears to act as a mechanical tie between contracted cells. Thus, attenuated processes of cytoplasm run from one cell to the nexus (Figs. 5 and 7), or processes from both cells meet at the nexus (Fig. 3). Often processes which appear close in one section lead to a nexus when followed in serial sections (Figs. 3 and 5). The nexus occurring where a process of one cell projects into another involves an extensive region of fusion as seen in Figs. 9, 10, and 13. The extent of the nexal area is apparent from a consideration of the tridimensional aspect of such projections as illustrated in Figs. 9 and 10.

FIGURE 7 Smooth muscle from the circular layer of cat small intestine which has been soaked in Krebs-Henseleit solution for 2 hours before fixation. This low-magnification electron micrograph demonstrates the large number of nexuses which can occur between smooth muscle cells. Two cells are interconnected by four nexuses in the lower portion of the field, while the central cell is fused, by means of a nexus, to the muscle cell in the upper portion of the field. The geometry of the cellular processes forming nexuses is altered by contraction of the cells during fixation, as evidenced by the bizarre shapes shown here. Permanganate-fixed, Araldite-embedded; section stained with uranyl acetate. × 16,000.

FIGURE 8 This electron micrograph illustrates at higher magnification the nexus shown at the arrow in Fig. 7. × 200,000.

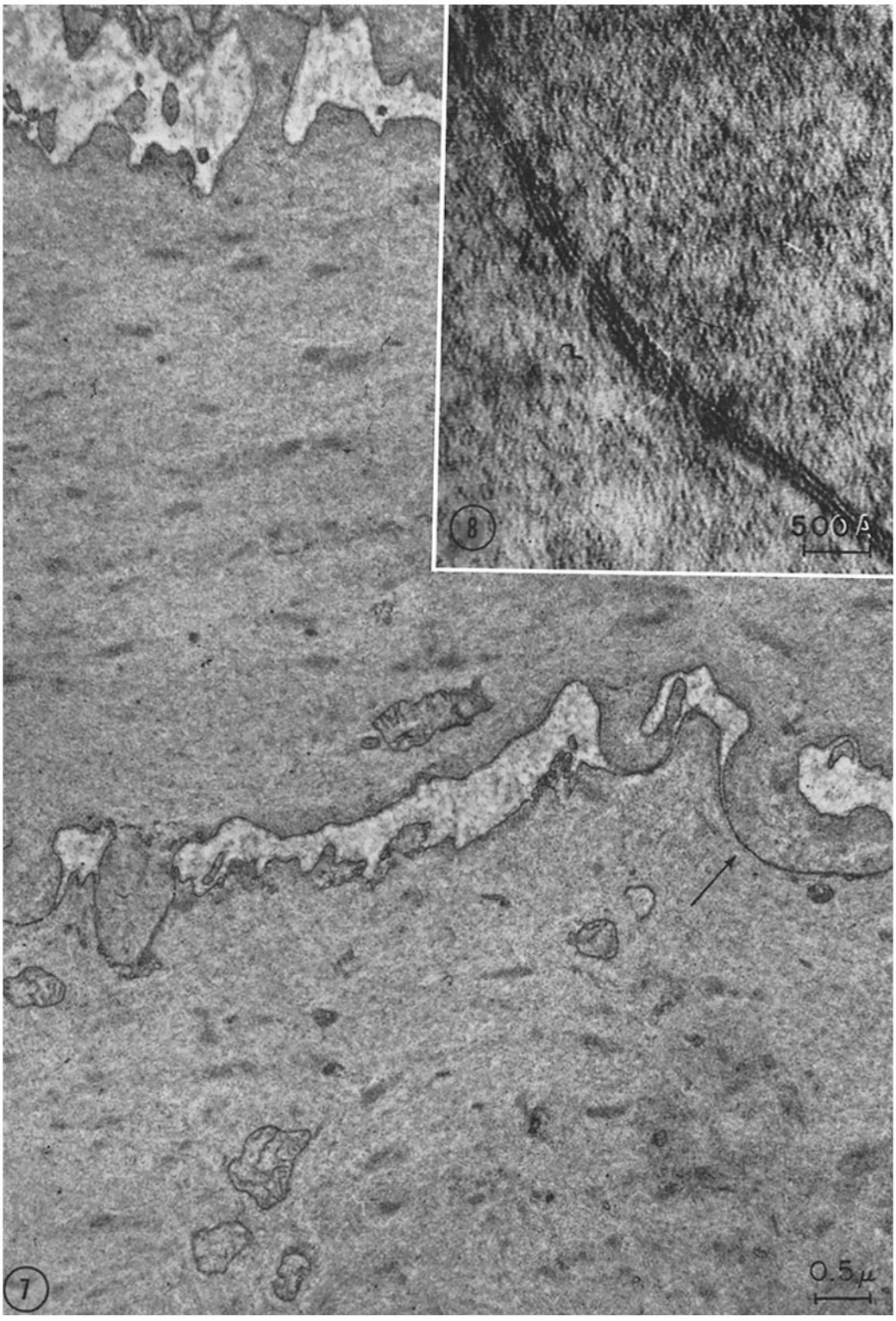
8
500 A
7
0.5 μ

The greatest area of nexus was seen in the projections of one cell into another in guinea pig smooth muscle. Moreover, nexuses could be observed in unincubated specimens. Nevertheless, the lability of the nexal structure is more easily seen at such regions than in nexuses of the abutment type. When the latter separates, no evidence of the existence of the nexus remains. However, one can see intermediate stages of nexal separation as illustrated by a comparison of Figs. 11 and 13 of guinea pig smooth muscle. In the former, the process seems to be retracted and the nexal regions restricted to a few residual spots (Fig. 12). This specimen was unincubated. In contrast, in an incubated preparation such a process (Figs. 13 and 14) is much larger and the nexus obtains over the entire surface of apposition.

Preliminary experiments with cat intestinal smooth muscle to which were applied contraction inhibitors, *i.e.* procaine, nitroglycerin, atropine, and low temperatures, indicate that when the fixation contraction is inhibited the nexuses are more often of the type seen in Figs. 9, 10, and 13.

In summary, then, while the region of nexus between smooth muscle cells can be visualized in specimens fixed in permanganate immediately upon extirpation, better preservation of the structure results from incubation before fixation and prevention of shortening. Further, in our experience with the muscles studied here, OsO_4 fixation provides no evidence of membrane fusion in smooth muscle.

Cardiac Muscle of Guinea Pig and Cat

For descriptive purposes, the intercalated disc of cardiac muscle can be subdivided into at least two regions, *i.e.* the interfibrillar and the intersarcoplasmic (Fig. 15). The interfibrillar portion is in the region of attachment of myofibrils to the adjacent plasma membranes of the disc. A gap of 100 to 200 A occurs between the plasma membranes at this region. The intersarcoplasmic portion of the intercalated disc, which may run in register with adjacent sarcomeres or move from one sarcomeric level to another, may be further subdivided into three distinctly different portions: (*1*) regions in which a 100 to 200 A gap occurs between adjacent membranes, (*2*) desmosomes, and (*3*) nexuses. The great extent of the nexus along the disc is illustrated in Fig. 15.

As in smooth muscle, the structure of the nexus of the intercalated disc is clearly seen after permanganate fixation. Figs. 16 and 18 (of OsO_4-fixed material) and Figs. 17 and 19 (of permanganate-fixed material) illustrate the structure of the nexus and its relation to structures within the cardiac muscle cells of the guinea pig. For example, Figs. 15 and 16 demonstrate that the plane of the nexus is usually parallel with the myofibrils. In all of the figures of OsO_4-fixed material, the light areas of the nexus are continuous with the gap between the plasma membranes and hence extracellular space. Therefore, from these micrographs alone, the central dark line could not be definitively identified as a region of fusion between adjacent plasma membranes. On the other hand, it is immediately apparent in high-magnification electron micrographs of permanganate-fixed preparations (Fig. 19) that the outer portions of adjacent plasma membranes fuse at the nexus. The thickness of the nexus in OsO_4-fixed cardiac muscle is quite variable and always

FIGURE 9 Smooth muscle from the circular layer of cat intestine which was soaked for 4 hours in Krebs-Henseleit solution prior to fixation. This electron micrograph illustrates a bulbous projection of one muscle cell into another. The plane of section passes parallel to the long axis of the projection. The adjacent cell membranes form a nexus throughout the extent of the invagination. Permanganate-fixed, Araldite-embedded; section stained with uranyl acetate. × 150,000.

FIGURE 10 Electron micrograph from the same specimen as shown in Fig. 9. This electron micrograph depicts a projection of one muscle cell into another, similar to that illustrated in Fig. 9. Here the plane of section passes transversely across the projection. As seen in enlargement (insert, × 320,000) of the area encircled, the membranes fuse to form a nexus. × 87,000.

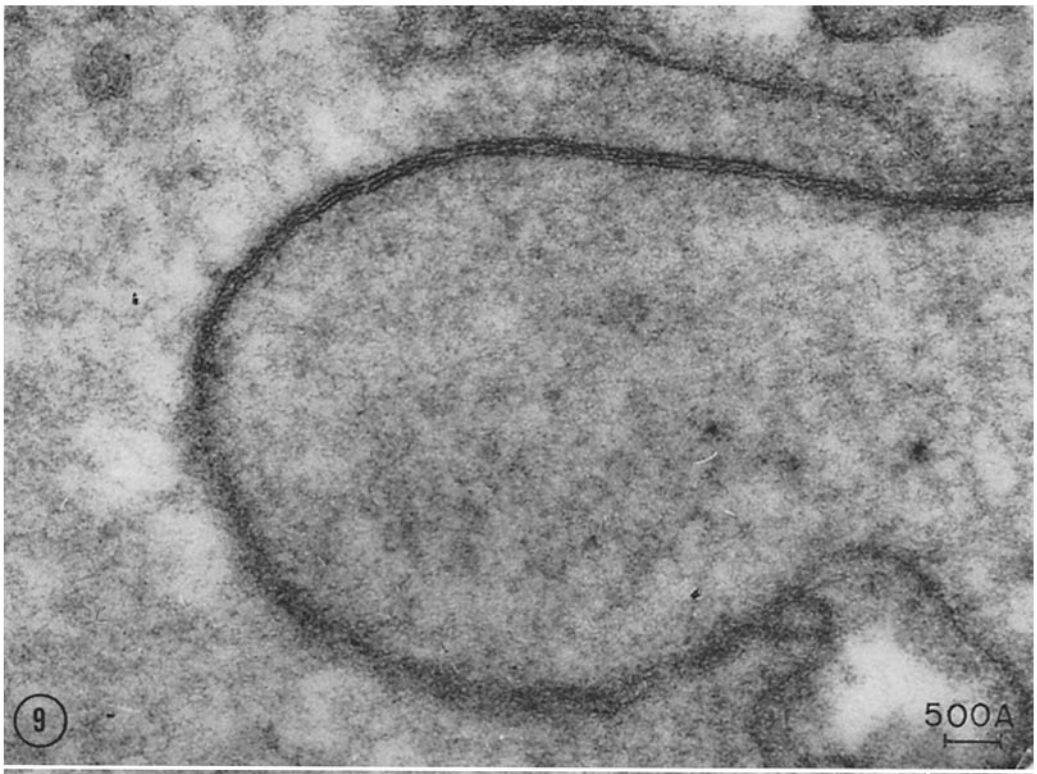
9
500A

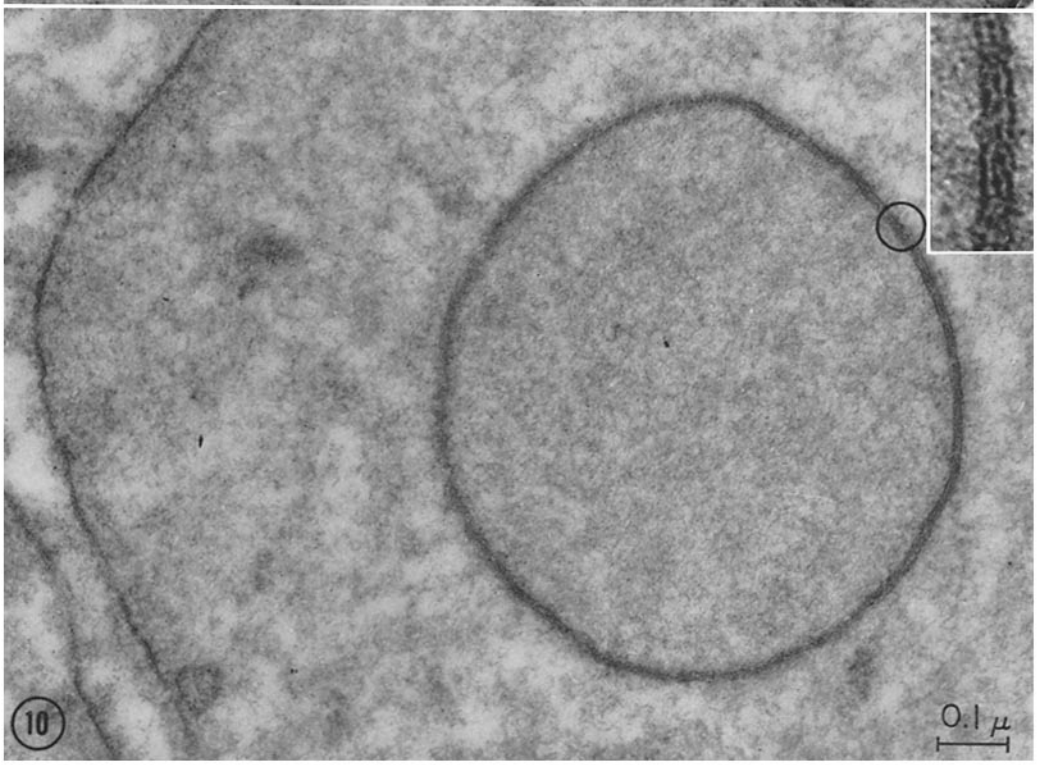
10
0.1 μ

equal to or greater than the thickness of the nexal regions of the disc in permanganate-fixed cardiac muscle (compare Figs. 18 and 19). Moreover, the three dark lines of the nexus in permanganate-fixed material are of uniform thickness, whereas in OsO_4-fixed material the nexus demonstrates marked asymmetry of the plasma membranes.

Figs. 20 and 21 illustrate the intercalated disc and nexus of the cardiac muscle of another species *i.e.* cat. The over-all organization of the disc and the structure of the nexus seem to be quite like those in cardiac muscle of the guinea pig.

From these studies it is apparent that the nexus along the intercalated disc of cardiac muscle is more readily demonstrable than the nexus in smooth muscle. While the nexus can be identified following OsO_4 fixation, evidence for actual fusion of membranes has been obtained only with permanganate fixation.

Median Giant Axon of Earthworm

The median giant axon of the earthworm is composed of neurons contributed by each segment. In the rostral portion of each segmental ganglion these neurons abut to form a septum. The plane of the septum makes an approximately 30° angle with the long axis of the nerve cord. Fig. 22 shows the septum in transverse section. The degree of myelination of the median giant axon is apparent in this micrograph. A previous study by Hama (24) of these junctions in OsO_4-fixed specimens was interpreted as demonstrating a gap between the septal membranes. In view of our experiences with OsO_4 and permanganate fixation for the study of cell contacts in smooth and cardiac muscles, it seemed reasonable to examine the membrane relations at the septate junctions in earthworm following permanganate fixation. The septum at its outer margin is illustrated in Fig. 23. Note that the extracellular space comes to an abrupt end as the plasma membranes of adjacent neurons are closely apposed. This close apposition extends across the septum. Where the plane of the septum is normal to the plane of section, as shown in Fig. 24, the cell membranes of adjacent neurons may be seen to form a nexus.

The data presented here clearly indicate that the neurons of the median giant axon of the earthworm are connected by nexal regions. This conclusion is strongly suggested even in OsO_4-fixed material. From both Hama's studies and the present study of OsO_4-fixed specimens, measure

FIGURE 11 Smooth muscle of guinea pig taenia coli fixed immediately after extirpation. This electron micrograph illustrates the more common form of intercellular relationship which is found in this smooth muscle, *i.e.* projection of a process of one cell into another cell. In this particular instance, the plasma membranes of adjacent cells do not form a continuous nexus through the extent of the intercellular relationship. It would appear that this process is pulling away from the other cell. This interpretation is supported by the fact that such a preparation shows maximal contraction during fixation. Permanganate-fixed, Araldite-embedded; section stained with lead. × 110,000.

FIGURE 12 An enlargement of the region encircled in Fig. 11. Note that the adjacent plasma membranes are separated by a considerable space for some distance, fuse to form a nexus, separate again, and then fuse again to form a nexus. × 280,000.

FIGURE 13 Smooth muscle of guinea pig taenia coli soaked for 45 minutes in Krebs-Henseleit solution prior to fixation. The bulbous projection of one muscle cell into another here is similar to that shown in Fig. 11. However, the adjacent cell membranes fuse throughout its length to form a nexus. The fact that this process is so much larger than the one illustrated in Fig. 11 would support the idea that the latter is being retracted due to contraction. Permanganate-fixed, Araldite-embedded; section stained with permanganate. × 44,000.

FIGURE 14 The region of nexus encircled in Fig. 13 photographed at higher magnification. Section stained with permanganate. × 270,000.

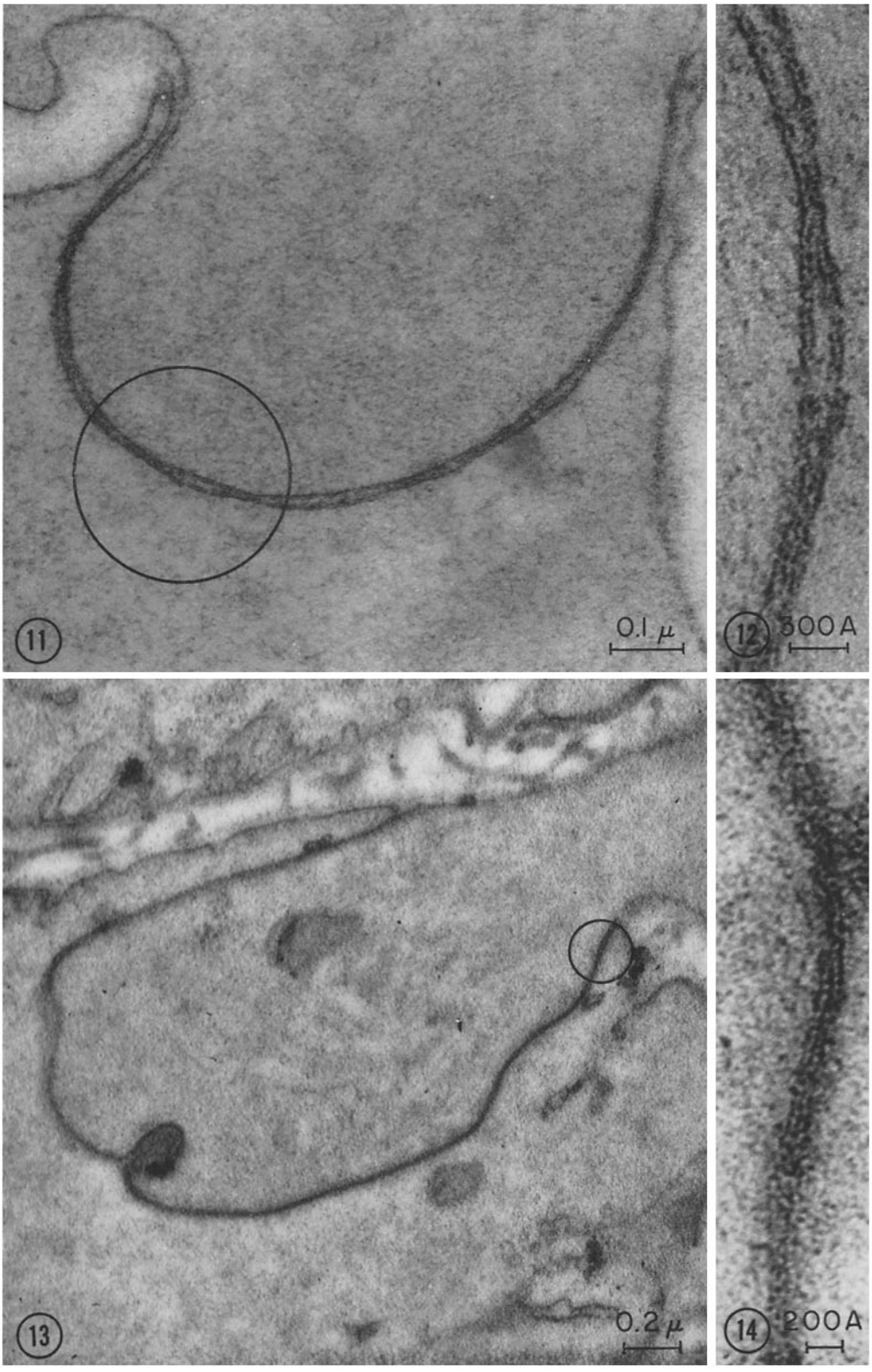
11
0.1 μ
12
300A
13
0.2 μ
14
200A

ments indicate that the thickness across the apposed membranes falls within the range of thickness of nexuses in other OsO_4-fixed tissues (see Table I). However, the outer leaflets of the cell membranes were not observed in OsO_4-fixed material in Hama's study or in this study; actual fusion of the membranes was demonstrated clearly only after permanganate fixation.

From the results obtained thus far on mammalian smooth and cardiac muscle and on earthworm axon, a direct correlation exists between electrotonic coupling and the occurrence of the nexus. Predicated on these findings, it seemed of value to determine whether a similar correlation could be obtained in various epithelia known to maintain transepithelial potentials. Thus, as examples of epithelia for which extensive physiological data are available frog skin and salivary gland epithelia were examined.

Frog Skin

In Fig. 25, the layers of frog epidermis and dermis are illustrated *i.e.* stratum corneum, stratum spinosum, stratum basale, and corium. The strata basale and spinosum are 4 to 6 cell layers thick, with the basal cell layer (stratum basale) composed of a prominent layer of columnar cells. The cells immediately above this layer are flattened in a manner characteristic of the remaining stratum spinosum. The area of abutment between adjacent cells of the basal layer is convoluted and contains few desmosomes (Fig. 26). A similarity is apparent between the regions of cell apposition in the stratum spinosum (Fig. 27) and the structure of the intercalated disc of cardiac muscle. Note the small extracellular space. The number of desmosomes and nexuses between the cells of the stratum spinosum and between these cells and the apical end of the basilar cells is much greater than along the side-to-side apposition of the basilar cells. Figs. 28 and 29 illustrate at high magnification the nexuses which occur between the squamous cells. In Fig. 28, especially, the association with desmosomes is apparent. These results corroborate the observations of Farquhar and Palade (35) on frog skin fixed with OsO_4. On the other hand, in our micrographs of frog skin fixed in isosmotic OsO_4 at room temperature, relatively large spaces are apparent between all the cells of the strata spinosum and basale (Fig. 30). No nexuses are present and the cells adhere to each other only at the desmosomes. That the cells are more adherent at desmosomes than at nexuses is consistent with our findings on other tissues as well as with the findings of Voute (36) and of Parakkal and Gedeon (37) on frog skin. In the stratum corneum we find, in agreement with Farquhar and Palade (35), that the nexuses are preserved by OsO_4 fixation.

Little doubt remains concerning the occurrence of nexuses between cells of the frog epidermis. The extent to which nexuses occur in the strata spinosum and basale, and whether they constitute an occluding zonule, however, is still indeterminant from a purely morphological point of view. Permanganate and OsO_4 give strikingly different pictures as regards the number of nexuses and the extent of intercellular space between cells of the strata spinosum and basale.

Submandibular Gland of the Rat

Nexuses occur between cells in both the acinar and ductular epithelia of rat submandibular

FIGURE 15 Guinea pig cardiac muscle fixed immediately after extirpation. A limited region of intercalated disc between two cells at a branch point of a cardiac muscle fiber is shown. The region of nexus along the disc is extensive (arrows). It occurs only in the regions of sarcoplasmic columns (intersarcoplasmic region of intercalated disc) as the disc passes from one sarcomeric level to another. Note that the adjacent plasma membranes form a nexus immediately upon turning in at the disc (near region at *ECS*). Where the disc crosses a sarcomere (interfibrillar region of intercalated disc), regions of attachment of myofilaments occur.

Desmosomes occur in the intersarcoplasmic regions of the disc. Two processes of the interdigitating region of the disc are seen in cross-section at *a* and *b*. OsO_4-fixed, Araldite-embedded; section stained with permanganate. × 31,000.


ECS
a
b
15
0.5 μ

gland (Figs. 31 to 36). The nexus is a part of the terminal bar. The number of desmosomes in the terminal bar may vary considerably. Further, in preparations in which considerable extraction has occurred (Figs. 31 to 33), the fibrillar nature of the cytoplasmic portion of the desmosome is apparent. Figs. 31 and 32 show this clearly for acinar cells and illustrate the order of occurrence along the terminal bar. The terminal bar of ductular epithelia is similar although it is often simpler; in particular, there seem to be fewer desmosomes as illustrated in Fig. 33. At high magnifications regions of nexal separation are sometimes visible (Fig. 34), reminiscent of unincubated guinea pig smooth muscle. Regions of nexuses and desmosomes together measure nearly 2 μ as Figs. 31 to 33 illustrate. Further, often an increased density of the cytoplasm immediately subjacent to the nexus is apparent, as is most clearly seen in Figs. 35 and 36. From these observations, then, it would seem probable that the entire complex constitutes the terminal bar (18). Even though it is possible to demonstrate the nexus in these epithelia fixed with OsO_4, the central line of fusion is not so dense as it is in epithelia fixed with permanganate. Thus the asymmetry of the membranes is evident here also.

The notion that the nexus does, in fact, form a girdle completely surrounding the apical ends of adjacent cells in epithelia has been proposed by Farquhar and Palade (18) who designated the girdle the *zonula occludens*. In sections which graze the ductular epithelium (Fig. 35), the nexus or *zonula occludens* can be seen to run from one portion of the lumen to another portion in which the lumen dips down between cells. Further, sections parallel to the cell axis always show a region of nexus associated with desmosomes between the apical ends of the cells (Figs. 31 to 33). In the rodent salivary glands, then, the lumen of both the ductular and acinar portions is presumably sealed off from the intercellular spaces by nexuses which form girdles or occluding zonules between acinar as well as ductular epithelial cells.

The nexuses between epithelial cells of the rodent submandibular gland, like those in the stratum corneum of frog skin but unlike those in the other tissues studied, are readily demonstrable with OsO_4 fixation. Even so, the asymmetry of the cell membranes is still apparent with this method.

In the order of presentation, the tissues examined in this study show a progression of decreasing differences between permanganate fixation and OsO_4 fixation. In smooth muscle, OsO_4 has not been useful so far in showing membrane

FIGURE 16 Guinea pig cardiac muscle fixed immediately after extirpation. A region of intercalated disc from the central portion of a cardiac muscle fiber is shown. The interfibrillar portion can be distinguished from the intersarcoplasmic portions of the disc by the insertion of the myofilaments into the disc. Desmosomes occur only in the intersarcoplasmic portions of the disc. The sarcoplasmic density adjacent to the inner leaflet of the plasma membrane at the desmosome appears to form a dark line immediately subjacent to the plasma membrane. The desmosome is easily distinguished from the nexus at the arrow. A relatively large intercellular space is apparent along the disc except at the nexus. The plasma membranes in the regions of the intercellular gap do not show triple layering. Only the cytoplasmic leaflet of the plasma membrane stains. OsO_4-fixed, Araldite-embedded; section stained with permanganate. × 76,000.

FIGURE 17 Guinea pig cardiac muscle fixed immediately after extirpation. This electron micrograph illustrates a region of the intercalated disc similar to that shown in Fig. 16. The same regions of the disc, interfibrillar and intersarcoplasmic, can be identified only with difficulty because of the lack of adequate preservation of the myofibrils by permanganate. However, about the same amount of extracellular space can be observed between the adjacent cell membranes of the disc except at the nexus (arrow). Permanganate-fixed, Araldite-embedded; section stained with uranyl acetate. × 45 000.


16
0.2 μ

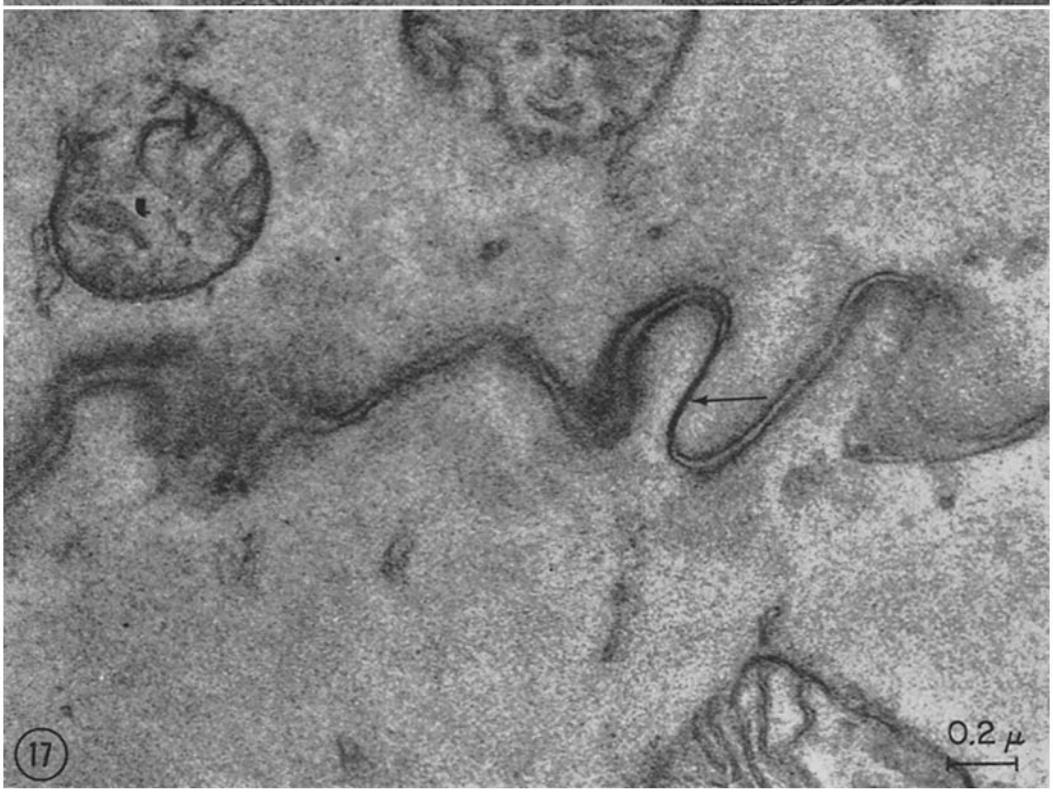
17
0.2 μ

fusion; for the tissues at the other end of this series, *i.e.*, salivary gland epithelia, one need use no other fixative.

DISCUSSION

The Distribution of the Nexus

Farquhar and Palade (18) have recently reviewed the literature on the nature and sites of fusion of adjacent cell membranes. The present report describes the distribution of the nexuses between mammalian smooth muscle cells, between mammalian cardiac muscle cells, between neurons of the median giant axon of earthworm, between cells of frog epidermis, and between cells of the acinar and ductular epithelia of rodent salivary gland.

Of particular interest is the apparent ease with which nexuses are demonstrated between epithelial cells after OsO_4 fixation. However, certain epithelia such as that of frog skin present experimental problems, as indicated by Voute (36) and Parakkal and Gedeon (37) and this report. When frog epidermis is fixed with OsO_4, relatively large spaces are apparent between the cells of the strata basale and spinosum and often between the ultimate and penultimate layers of the strata corneum and spinosum. Farquhar and Palade (35) reported the occurrence of such "lakes" only in the strata spinosum and germinativum. However, data presented here on permanganate-fixed epidermis show little intercellular space throughout the epithelium, rarely exceeding 200 A, and more numerous nexuses between cells of all layers. These divergent observations illustrate the vagaries of fixation and indicate the need for experimental resolution of the differences.

The question of the existence of nexuses in nervous tissue, *i.e.* between neurons, between neurons and glial elements, and between glial cells, is particularly relevant. Such structures have been described by Robertson (8) in the median-to-motor synapse of the crayfish (here called external compound membrane), between myelin sheaths and glial cells in the optic nerve (38), and between glial processes surrounding cerebral capillaries (39). Recently, Robertson *et al.* (5) and Robertson (6) have described a neuron-to-neuron contact at the synapses on the lateral dendrite of the Mauthner cell of the goldfish. Contacts such as these may be different from simpler fusions in that they show a two-dimensional periodic substructure in the plane of fusion. Also, Bennett *et al.* (7) have reported evidence for electrotonic coupling at a spinal synapse in Mormyrid electric fish and have shown special regions between the neurons. Using OsO_4, they concluded that these regions are areas of membrane fusion. In fact, when compared at the same magnification, these regions and the nexal regions described here along the intercalated discs of OsO_4-fixed mammalian cardiac muscle show the same structure. In summary, it may be that all these sites of fusion are, in fact, nexuses.

Unfortunately, there is not, as yet, a one-to-one correspondence between the occurrence of the nexus and cell-to-cell electrotonic spread. There are at least four other areas in which one might predict, on the basis of electrophysiological data, the occurrence of nexuses: (*1*) the septate junctions in the median giant axon of the earthworm (24); (*2*) the septate junctions in the lateral giant fiber of the crayfish (25); (*3*) the lateral-to-motor synapse in the crayfish (25); and (*4*) between glial

FIGURE 18 Guinea pig cardiac muscle fixed immediately after extirpation. A nexal region of an intercalated disc is depicted. Fusion of the outer lamellae of adjacent plasma membranes is apparent. The central dark line representing the fused outer leaflets of adjacent plasma membranes is narrow and beaded in appearance after OsO_4 fixation. This is in contrast to the heavily stained, broader leaflets on the cytoplasmic side of each plasma membrane. OsO_4-fixed, Araldite-embedded; section stained with uranyl acetate. × 260,000.

FIGURE 19 An enlargement of Fig. 17. Note the uniformity of dark and light lines in the region of nexus. The central dark line has the same dimension as either of the outer dark lines. × 440,000.

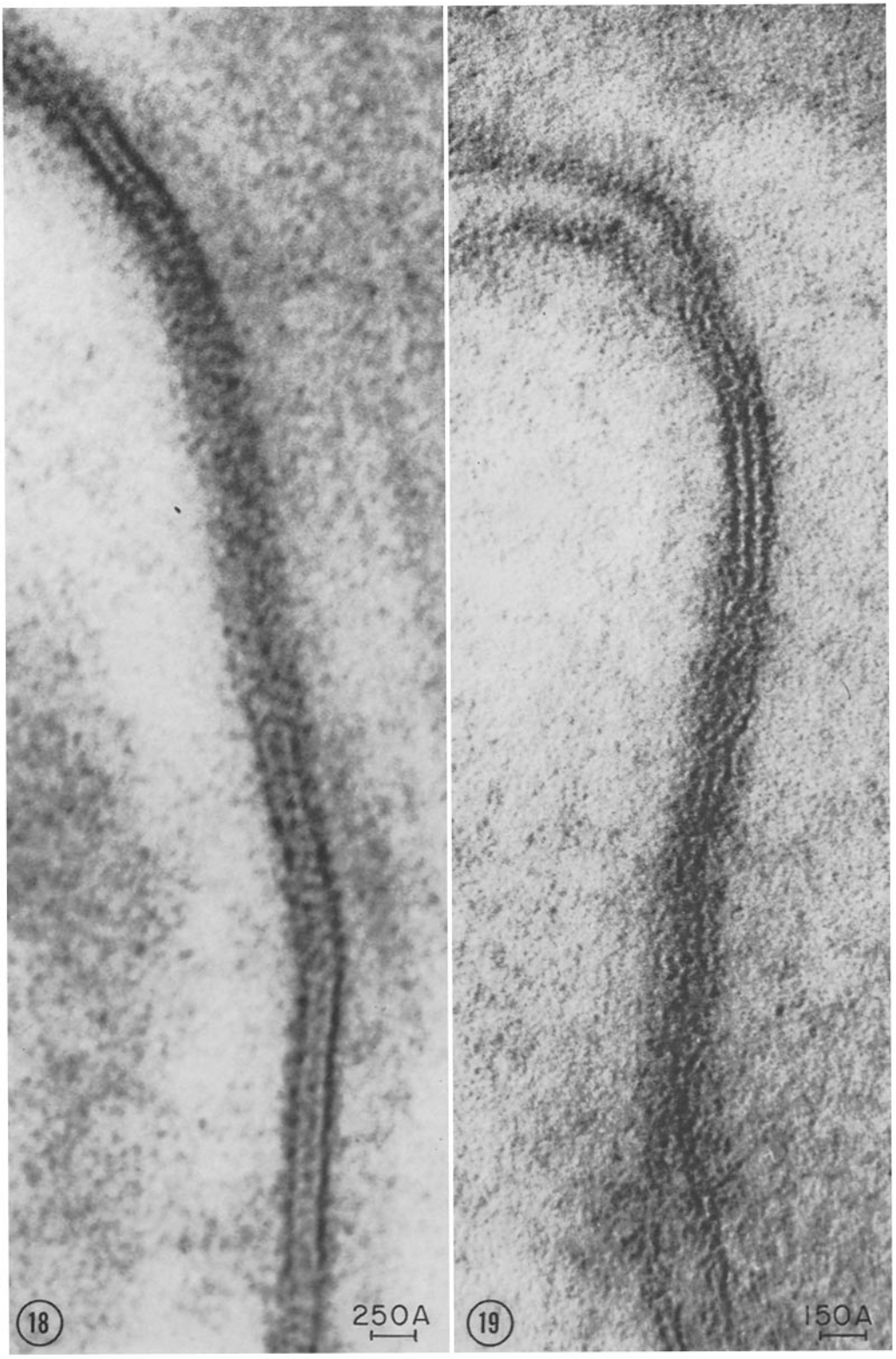
18
250A
19
150A

cells in the central nervous system of the leech (26). All four of these areas have been studied recently and no nexuses have been reported. It is interesting to note, in light of the above discussion, that all of these studies were based on observations of OsO_4-fixed material.

When, however, the septate junction of the median giant axon of the earthworm was studied following permanganate fixation, a nexus between the neurons was clearly evident. Preliminary studies on the crayfish synapses show similar results. Coggeshall and Fawcett (26) did not find areas of fusion between glial cells in the leech even though the work of Kuffler and Potter (40), as they suggested, indicates strongly that regions of special contact between glial cells do occur. There are no published reports on the appearance of these glial interconnections after permanganate fixation.

The occurrence of a nexal type structure along the intercalated disc of cardiac muscle was suggested over a decade ago (41). Early electron microscope studies gave only an indication of such areas involving fusion along the disc (3). Karrer (4), by extrapolating from studies on cervical epithelium where fusion of cell membranes was clear because the outer leaflets of each membrane were visible, interpreted the central line in his "quintuple-layered cell interconnection" as a region of fusion. Again, unequivocal conclusions could be reached only after such areas had been visualized following permanganate fixation which permitted the identification of all layers of each cell membrane at the region of fusion.

Structure and Dimension of the Nexus

Table I summarizes measurements (cytoplasmic leaflet to cytoplasmic leaflet inclusive) of the thickness of the nexuses illustrated in this report and shows the consistency of these measurements on permanganate-fixed material. The ability of permanganate to preserve membrane structure with such uniformity is especially valuable when this fixative is used in a comparative study of the nexus. Unfortunately, the chemical moieties within the plasma membrane which are stabilized and stained by permanganate have yet to be elucidated (42).

Measurements of nexuses in OsO_4-fixed material range upward from the 125 to 150 A, characteristic of nexuses in permanganate-fixed material, to as high as 250 A. Several factors presumably contribute to this. While OsO_4 consistently stains the cytoplasmic lamella, it variably does or does not stain the outer lamella of the plasma membrane in certain tissues (16, 42, and this report) even when sections are subsequently stained with heavy metals. However, that the outer lamella of the plasma membrane in various epithelia is preserved, although not always stained by OsO_4, has been clearly demonstrated here and elsewhere (16, 18, 42). Whether this is tissue-dependent (*i.e.* represents actual molecular differences between plasma membranes of different cells or along membranes of the same cell) or merely represents quality of preservation (as a function of time of fixation, temperature of fixation, osmolarity of fixative, embedding media, etc.) is, from experience gained in this laboratory and from surveying the literature, indeterminate. It could be argued, however, from the physiological viewpoint, that differences in chemical composition of the membrane may be the decisive factor (43).

The fact that, in some cases, the outer lamella may not be well preserved by OsO_4 could result in a lack of adherence of the membranes at the

FIGURE 20 Cat cardiac muscle fixed immediately upon extirpation. The intercalated disc of cat cardiac muscle is similar to that of guinea pig cardiac muscle, as illustrated by this micrograph. The nexus (at the arrow) occurs along the intersarcoplasmic portions of the disc usually where it passes from one sarcomeric level to another. Desmosomes (*a* and *b*) occur in the internexal region. Permanganate-fixed, Araldite-embedded; section stained with uranyl acetate. × 20,000.

FIGURE 21 A higher magnification of the nexus illustrated in Fig. 20. The nexus shows remarkable uniformity of structure throughout its length. Section stained with uranyl acetate. × 230,000.


a
b
20
0.5 μ
21
300A

TABLE I

Thickness of Nexus

Tissue	Thickness	Fixative	Figure
	Angstrom Units		
Intestinal smooth muscle			
Dog	155	Permanganate	(Ref. 1)
	145	Permanganate	4
	145	Permanganate	6
Cat	120	Permanganate	8
	130	Permanganate	9
	130	Permanganate	10
Guinea pig	125	Permanganate	12
	140	Permanganate	14
Cardiac muscle			
Guinea pig	190	OsO_4	16
	230	OsO_4	18
	140	Permanganate	19
Cat	125	Permanganate	21
Septum of median giant axon			
Earthworm	170	Permanganate	24
Frog skin	130	Permanganate	29
Submandibular gland			
Rat	135	OsO_4	34
	160	OsO_4	36

nexus during subsequent treatment. This may be the explanation for the lack of demonstration of nexuses in OsO_4-fixed smooth muscle preparations even after staining with various heavy metals. Another factor contributing to variations in preparations fixed with OsO_4 is the variation in thickness of the cytoplasmic lamella (42). Comparison of Figs. 16, 18, 34, and 36 makes apparent the difference in thickness of the cytoplasmic lamellae. In any event, the present variations in fixation, subsequent treatment of tissues, and tissue types make evident the need for well controlled experi-

FIGURE 22 A photomicrograph of a cross-section of the earthworm nerve cord. The septum is seen as a wavy line across the median giant axon. Bouin's-fixed, celloidin-embedded; Masson trichrome-stained. × 400.

FIGURE 23 This electron micrograph demonstrates the extent of the close apposition of the plasma membranes of adjacent nerve cells across the septum. Arrow marks extracellular space in the lateral portion of the septum. Permanganate-fixed, Araldite-embedded; section stained with permanganate. × 18,000.

FIGURE 24 An electron micrograph of much higher magnification of the encircled region in Fig. 23. The two plasma membranes of adjacent neurons come together and form a long nexus. The characteristic three dark lines of the nexus can be distinguished at the several places encircled in which the membranes are sectioned normal to the plane of the septum. Section stained with permanganate. × 350,000.

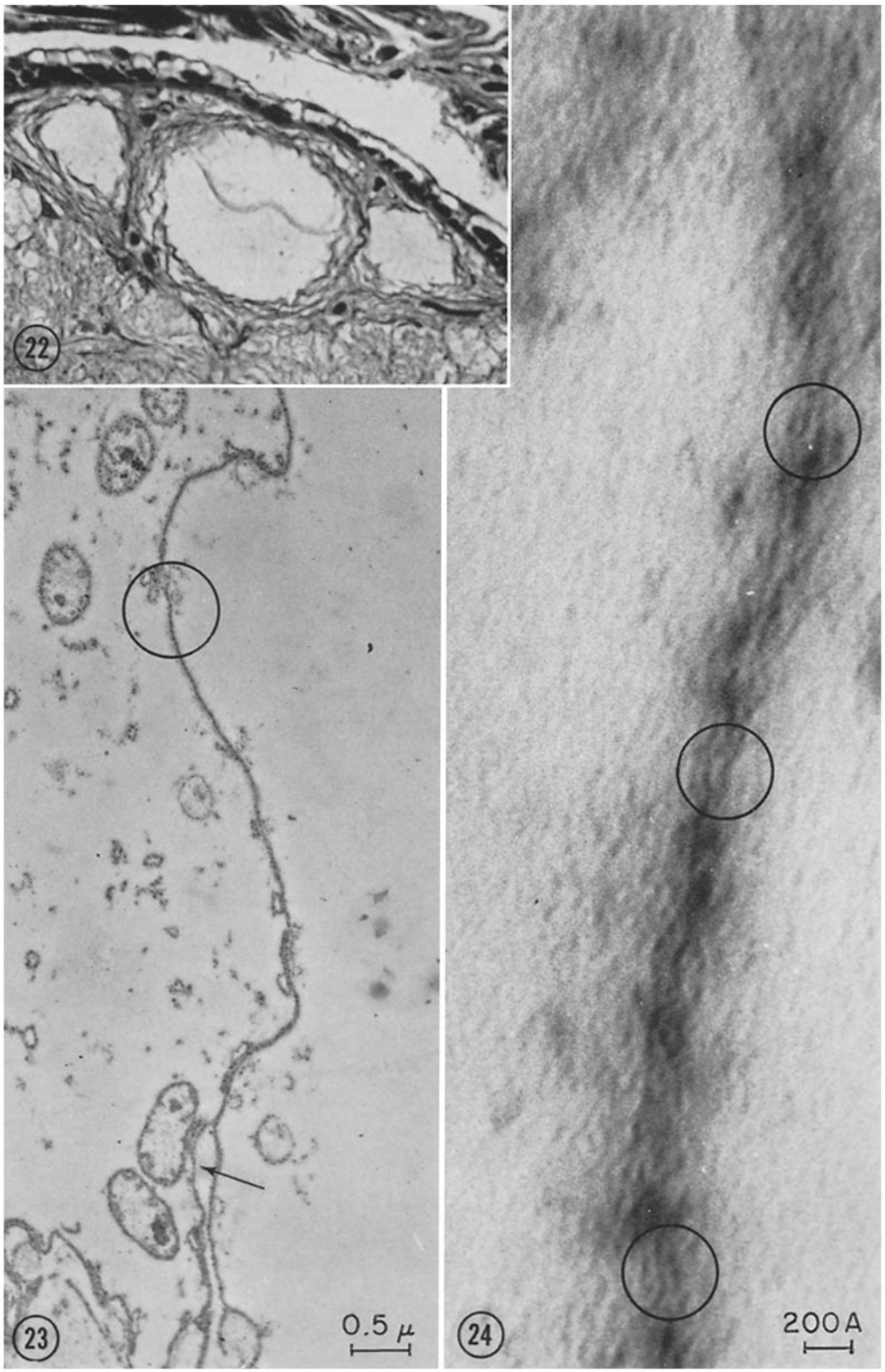
22
23
0.5 μ
24
200A

mental comparisons between nexuses in OsO_4-fixed and permanganate-fixed tissues.

Stoeckenius (44, 45) has demonstrated that the hydrophilic ends of phospholipids react with OsO_4 to become electron opaque in fixed material. Further, he has demonstrated that the addition of protein layers to a bimolecular leaflet of lipid molecules in model systems results in a structure similar to the plasma membrane as seen in sectioned material. Such evidence adds strong support to the pauci-molecular theory of plasma membrane structure as proposed by Davson and Danielli (46).

On the basis of the Davson-Danielli model, tentative suggestions regarding the molecular structure of the nexus may be made. First, because of the reversibility of the formation of the nexus and the loss of the thickness of one outer lamella, it is possible that the membrane fusion at the nexus is due to interdigitation of ionic groups. Second, since the electron-transparent region of the fixed membrane is unaltered at the nexus, it appears that the lipid layers of the membrane are relatively undisturbed at these nexuses. Third, any water molecules present in the nexus are probably strongly bound.

Robertson (8) has pointed out several ways that cell membranes may interact, with a resulting local loss of membrane components. However, in view of the reversibility of the nexus, actual loss of material from the membrane seems unlikely.

The Possible Functional Roles of the Nexus

The problems of impulse propagation in smooth muscle (2, 47), cardiac muscle (48, 49), and earthworm median giant axon (50) have been reviewed recently. In each case, quantitative evidence for appreciable electrotonic coupling is available (47, 48, 51, 52), and there is electrical transmission of action potentials from one cell to another. Whether the current responsible for transmission flows across the nexus or across a region in which there is an extracellular gap remains to be demonstrated experimentally.

However, there are several arguments in favor of the former assumption. First, the nexus provides a possibility for electrotonic current spread ahead of the propagating action potential unattenuated by current shunt *via* an intercellular gap. That intercellular gaps as narrow as 100 A can effectively isolate cells has been demonstrated (53–55). Second, the driving voltage for a current line through a nexal region is the difference between the pre-cell and the post-cell membrane potential, while the driving voltage for a line across any gap between cells is the difference of membrane potential along the pre-cell membrane. To illustrate, consider a hypothetical situation in which the pre-cell membrane has one voltage across it everywhere and the post-cell membrane has another. Obviously, current would flow by way of the nexus but not across gap regions.

In any case, the amount of current flowing between the cells is, of course, dependent on the resistance of the coupling structures. Electrical measurements indicate that the membranes at the sites of electrotonic coupling are of relatively low resistance regardless of the geometry of their apposition. Independent evidence indicating this has been obtained by demonstrating a functionally direct pathway between cardiac cell interiors for the movement of K^{42} (49). In this regard, it should be noted that membranes at the nexus are exposed on both sides to high potassium and low calcium concentrations and are probably depolarized. All these factors are associated in other cir-

FIGURE 25 A photomicrograph of frog skin. The following layers are illustrated: stratum corneum, stratum spinosum, stratum basale, and corium. Figs. 26 to 30 are all taken from either the basal columnar layer or the upper 2 to 3 layers of squamous cells of the stratum spinosum (between arrows). Bouin's-fixed, celloidin-embedded; stained with Masson's trichrome. × 650.

FIGURE 26 An electron micrograph of frog skin showing cells of the stratum basale. The basilar columnar cells are very closely apposed, with extracellular space discernible only at intervals. A prominent basement membrane can be seen. Permanganate-fixed, Araldite-embedded; section stained with permanganate. × 15,000.

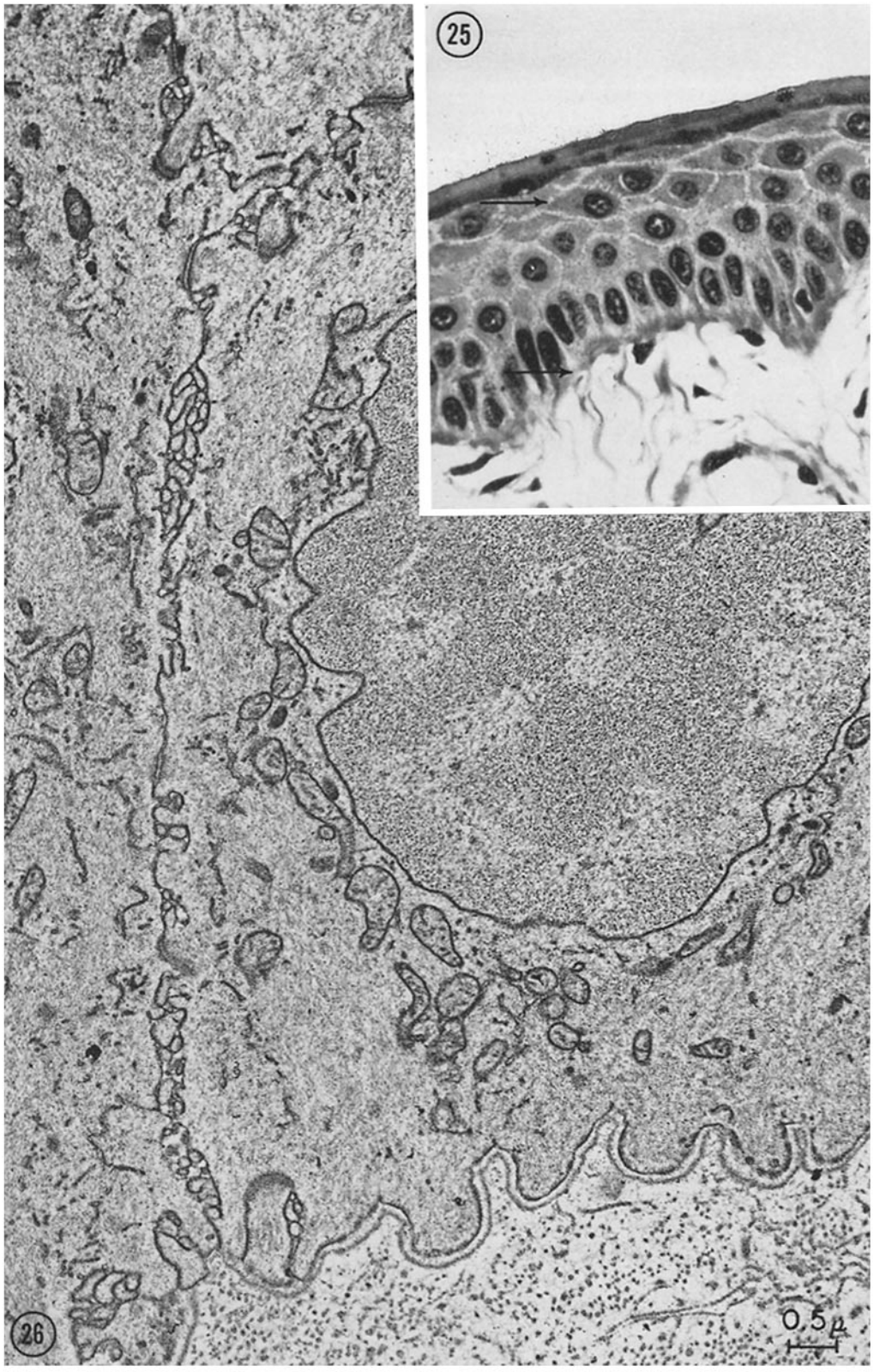
25
26
0.5 μ

cumstances with decreased membrane resistance. Nevertheless, the membranes of the nexus certainly have a larger resistance than the equivalent volume of cytoplasm. If the nexuses are the electrically important connections between cells, the internal resistance due to them, beyond that of the myoplasm, may account for the relatively short length constants and slow rates of propagation in some involuntary muscle.

Finally, it has been reported recently that both the nexal area and electrotonic coupling between atrial cells of the heart are decreased by hypertonic sucrose solutions. In hypotonic sucrose, electrical coupling is increased and the nexal area is increased or normal. This provides strong experimental evidence to support the hypothesis that nexuses can be sites of electrotonic coupling between cells (56). Hypertonic sucrose solution also decreases electrotonic spread in rat atrium (48).

At the same time that fusion of cell membranes at the nexus provides a pathway for movement of material normal to the membranes (*i.e.* from one cell interior to another), it also cuts off movement of matter tangent to the membrane. Since terminal bars are usually associated with the barrier to diffusion across epithelia, it has been suggested repeatedly that the lack of extracellular space is the cause of the block to diffusion as opposed to the presence of some obstructing extracellular cement substance. Farquhar and Palade (18) have demonstrated that the barrier to protein molecules in kidney tubules and pancreatic acini and ducts is the region of fusion of adjacent cell membranes in the terminal bar which they call a "tight junction." The terms "tight junction" and "nexus" refer to the same morphological structure. The difference in terms lies in their implicit reference to the two functional correlates of the membrane fusion. In epithelia, however, the nexus may play both roles. Recently Kanno and Loewenstein (57) have demonstrated a low-resistance diffusion pathway between cell interiors of the salivary gland of *Drosophila*. They have also reported special regions of contact between the cells. In the frog skin it would appear that the nexuses of the strata corneum, spinosum, and basale may allow electrolytes and metabolites to pass between cell interiors. It would be pertinent to determine whether cells of the frog epidermis and other epithelia have low-resistance interconnections.

Part of this work presented at the 76th Annual Meeting of the American Association of Anatomists, Washington, D. C., April 9–11, 1963.

This investigation was supported by research grants A-3449 and A-3819 from the National Institutes of Health, United States Public Health Service.

Received for publication, May 29, 1963.

REFERENCES

1. DEWEY, M. M., and BARR, L., Intracellular connection between smooth muscle cells: the nexus, *Science*, 1962, **137**, 670.
2. BARR, L., Propagation in vertebrate visceral smooth muscle, *J. Theoret. Biol.*, 1963, **4**, 73.
3. SJÖSTRAND, F. S., ANDERSSON-CEDERGREN, E., and DEWEY, M. M., The ultrastructure of the intercalated discs of frog, mouse and guinea pig cardiac muscle, *J. Ultrastruct. Research*, 1958, **1**, 271.
4. KARRER, H. E., The striated musculature of blood vessels. II. Cell interconnections and cell surface, *J. Biophysic. and Biochem. Cytol.*, 1960, **8**, 135.
5. ROBERTSON, J. D., BODENHEIMER, T. S., and STAGE, D. E., The ultrastructure of Mauthner cell synapses and nodes in goldfish brains, *J. Cell Biol.*, 1963, **19**, 159.
6. ROBERTSON, J. D., The occurrence of a subunit pattern in the unit membranes of club endings in Mauthner cell synapses in goldfish brains, *J. Cell. Biol.*, 1963, **19**, 201.

FIGURE 27 This electron micrograph overlaps with Fig. 26. The squamous cells are apposed to each other along a ragged boundary which is quite similar to the intercalated disc of cardiac muscle. Nexuses, indicated by arrows, alternate, along the boundary, with desmosomes and are in fact usually adjacent to them (see Figs. 28 and 29). Note that the desmosomes are much rarer along the boundary between the columnar cells (stratum basale) (*a*) as are the nexuses. × 9,400.

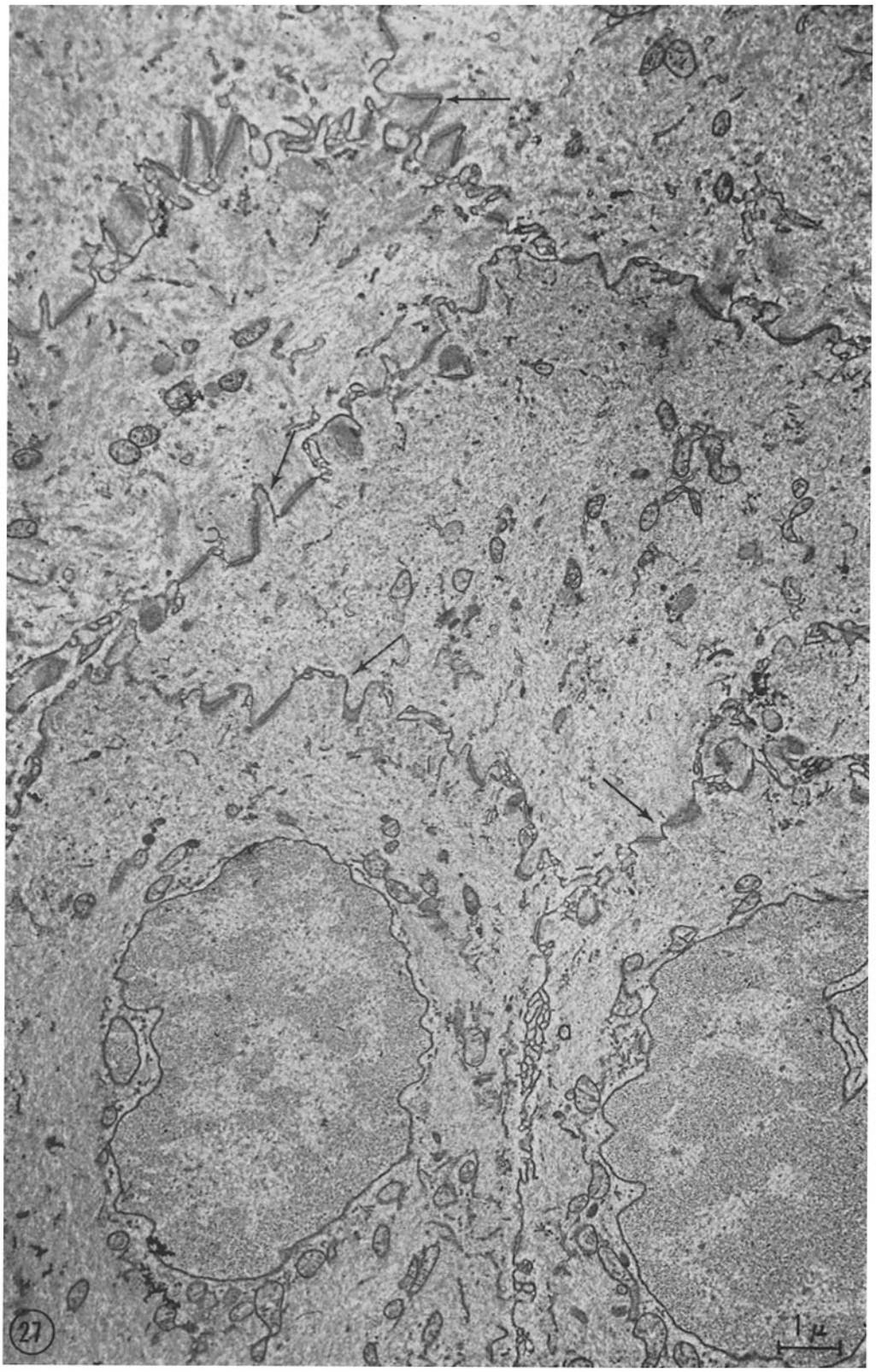
27
1 μ

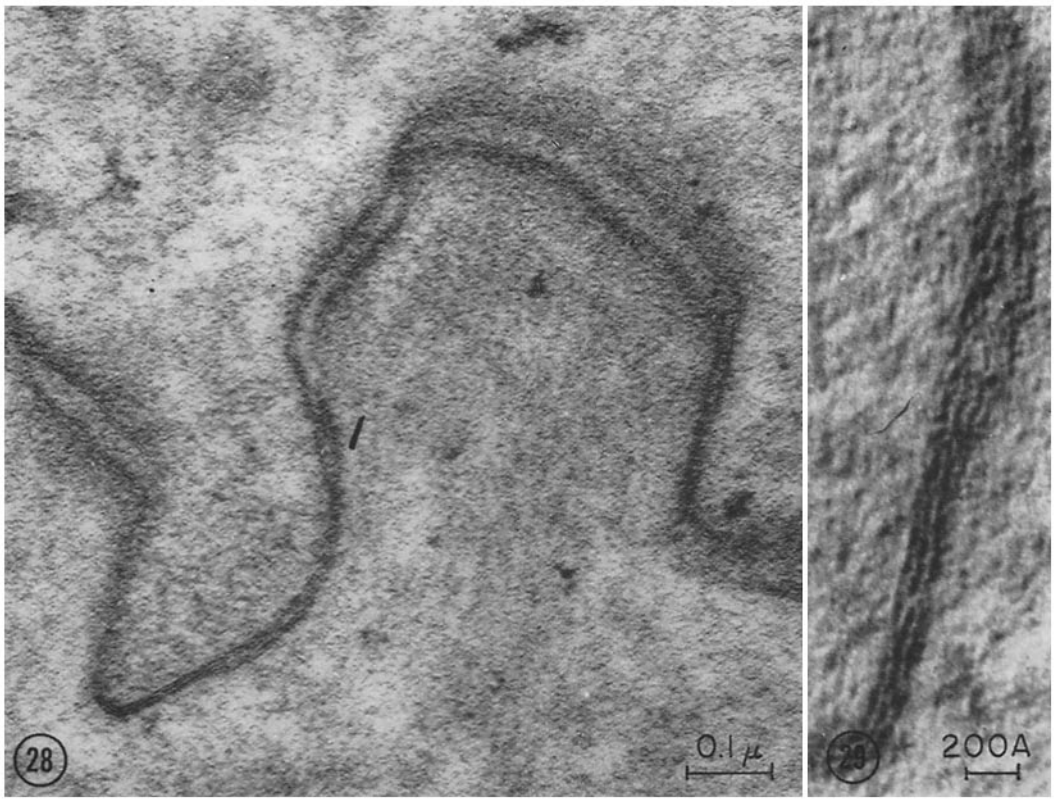

FIGURE 28 An electron micrograph of frog skin showing nexuses as they occur in close relation to desmosomes at the boundary between the squamous cells of the stratum spinosum. Permanganate-fixed, Araldite-embedded; section stained with permanganate. × 110,000.

FIGURE 29 An enlargement of the nexus at the lower left of Fig. 28. × 350,000.

7. BENNETT, M. V. L., ALJURE, E., NAKAJIMA, Y., and PAPPAS, G. D., Physiological and morphological characterization of an electrotonic junction between teleost spinal neurons, *Science*, 1963, **141,** 262.
8. ROBERTSON, J. D., Ultrastructure of excitable membranes and the crayfish median-giant synapse, *Ann. New York Acad. Sc.*, 1961, **94,** 339.
9. BERGMAN, R. A., Intercellular bridges in ureteral smooth muscle, *Johns Hopkins Hosp. Bull.*, 1958, **102,** 195.
10. PROSSER, C. L., BURNSTOCK, G., and KAHN, J., Conduction in smooth muscle: comparative structural properties, *Am. J. Physiol.*, 1960, **199,** 545.
11. HARMAN, J. W., O'HEGARTY, M. T., and BYRNES, C. K., The ultrastructure of human smooth muscle. Studies of cell surface and connections in normal and achalasia esophageal smooth muscle, *Exp. Molec. Path.*, 1962, **1,** 204.
12. EVANS, D. H. L., and EVANS, E. M., The membrane relationships of smooth muscles: an electron microscope study, *J. Anat.*, London, 1964, **98,** 37.
13. KARRER, H. E., Cell interconnections in normal human cervix epithelium, *J. Biophysic. and Biochem. Cytol.*, 1960, **7,** 181.
14. CHOI, J. K., The fine structure of the urinary bladder of the toad, *Bufo marinus*, *J. Cell Biol.*, 1963, **16,** 53.
15. ITO, S., and WINCHESTER, R. J., The fine structure of the gastric mucosa in the bat, *J. Cell Biol.*, 1963, **16,** 541.
16. SJÖSTRAND, F. S., and ELFVIN, L. G., The layered, asymmetric structure of the plasma membrane in the exocrine pancreas cells of the cat, *J. Ultrastruct. Research*, 1962, **7,** 504.
17. SJÖSTRAND, F. S., The ultrastructure of the plasma membrane of columnar epithelium cells of the

FIGURE 30 An electron micrograph of an area of frog skin similar to that demonstrated in Fig. 27. This electron micrograph illustrates the relatively large extent of intercellular space present after OsO_4 fixation of the epidermis. The cells appear adherent to each other only at the desmosomes. The space between cells extends throughout the basilar columnar layer as well as between the ultimate and penultimate layers of the epidermis. OsO_4-fixed, Epon-embedded; section stained with uranyl acetate and lead. × 9600.

mouse intestine, *J. Ultrastruct. Research*, 1963, **8,** 517.

18. FARQUHAR, M. G., and PALADE, G. E., Junctional complexes in various epithelia, *J. Cell Biol.*, 1963, **17,** 375.
19. ROBERTSON, J. D., The molecular structure and contact relationships of cell membranes, *Progr. Biophysics and Biophysic. Chem.*, 1960, **10** 343.
20. FARQUHAR, M. G., and PALADE, G. E., Tight intercellular junctions, First Annual Meeting of American Society of Cell Biology, 1961, 57, abstract.
21. CAESAR, R., EDWARDS, G. A., AND RUSKA, H., Architecture and nerve supply of mammalian smooth muscle tissue, *J. Biophysic. and Biochem. Cytol.*, 1957, **3,** 867.
22. RHODIN, J. A. G., Fine structure of vascular walls in mammals, *Physiol. Rev.*, 1962, **45,** suppl. 5, 48.
23. MERRILLEES, N. C. R., BURNSTOCK, G., and HOLMAN M. E., Correlation of fine structure and physiology of the innervation of smooth muscle in the guinea pig vas deferens, *J. Cell Biol.*, 1963, **19,** 529.
24. HAMA, K., Some observations on the fine structure of the giant nerve fibers of the earthworm, *Eisenia foetida*, *J. Biophysic. and Biochem Cytol.*, 1959, **6,** 61.
25. HAMA, K., Some observations on the fine structure of the giant fibers of the crayfishes (*Cambarus virilus* and *Cambarus clarkii*) with special reference to the submicroscopic organization of the synapses, *Anat. Rec.*, 1961, **141,** 275.
26. COGGESHALL, R. E., and FAWCETT, D. W., The fine structure of the central nervous system of the leech, *Hirudo medicinalis*, *J. Neurophysiol.*, 1964, **27,** 229.
27. KREBS, H. A., and HENSELEIT, K. Untersuchungen über die Harnstoffbildung im Tierkörper, *Z. Physiol. Chem.*, 1932, **33,** 210.
28. PALADE, G. E., A study of fixation for electron microscopy, *J. Exp. Med.*, 1952, **95,** 285.

29. LUFT, J. H., Permanganate—a new fixative for electron microscopy, *J. Biophysic. and Biochem. Cytol.*, 1956, **2,** 799.
30. KURTZ, S. M., A new method for embedding tissues in Vestopal W, *J. Ultrastruct. Research*, 1961, **5,** 468.
31. LUFT, J. H., Improvements in epoxy resin embedding methods, *J. Biophysic. and. Biochem. Cytol.*, 1961, **9,** 409.
32. KARNOVSKY, M. J., Simple methods for "staining with lead" at high pH in electron microscopy, *J. Biophysic. and Biochem. Cytol.*, 1961, **11,** 729.
33. LAWN, A. M., The use of potassium permanganate as an electron-dense stain for sections of tissue embedded in epoxy resin, *J. Biophysic. and Biochem. Cytol.*, 1960, **7,** 197.
34. WATSON, M. L., Staining of tissue sections for electron microscopy with heavy metals, *J. Biophysic. and Biochem. Cytol.*, 1958, **4,** 475.
35. FARQUHAR, M. G., AND PALADE, G. E., Functional organization of amphibian skin, *Proc. Nat. Acad. Sc.*, 1964, **51,** 569.
36. VOUTE, C. L., An electron microscopic study of the skin of the frog (*Rana pipiens*), *J. Ultrastruct. Research*, 1963, **9,** 497.
37. PARAKKAL, P. F., AND GEDEON, M. A., A study of the fine structure of the epidermis of *Rana pipiens*, *J. Cell Biol.*, 1964, **20,** 85.
38. PETERS, A., Plasma membrane contacts in the central nervous system, *J. Anat.*, 1962, **96,** pt. 2, 237.
39. GRAY, E. G., Ultra-structure of synapses of cerebral cortex and of certain specializations of neuroglial membranes, *in* Electron Microscopy in Anatomy, (J. D. Boyd, F. R. Johnson, and J. D. Lever, editors), London, Edward Arnold and Co., 1961, 54.
40. KUFFLER, S. W., and POTTER, D. D., Glia in the leech central nervous system: physiological properties in neuron-glia relationship, *J. Neurophysiol.*, 1964, **27,** 290.
41. CURTIS, H. J., and TRAVIS, D. M., Conduction in Purkinje tissue of the ox heart, *Am. J. Physiol.*, 1951, **165,** 173.
42. SJÖSTRAND, F. S., Morphology of ordered biological structures, *Radiation Research*, (L. G. Augenstine, editor), 1960, New York and London, Academic Press, Inc., suppl., **2,** 349.
43. DEWEY, M. M., The ultrastructure of mammalian cell membranes, *Univ. Mich. Med. Bull.*, 1959, **25,** 132.
44. STOECKENIUS, W., Some electron microscopical observations on liquid-crystalline phases in lipid-water systems, *J. Cell Biol.*, 1962, **12,** 221.
45. STOECKENIUS, W., The molecular structure of lipid-water systems and cell membrane models studied with the electron microscope, *in* The Interpretation of Ultrastructure, Symposium International Society for Cell Biology, (R. J. C. Harris, editor), New York and London, Academic Press, Inc., 1962, 349.
46. DAVSON, H., and DANIELLI, J. F., The Permeability of Natural Membranes, 2nd edition, Cambridge, University Press, 1952.
47. NAGAI, T., and PROSSER, C. L., Electrical parameters of smooth muscle cells, *Am. J. Physiol.*, 1963, **204,** 915.
48. WOODBURY, J. W., and CRILL, W. E., On the problem of impulse conduction in the atrium, *in* Nervous Inhibitions, 1961, Oxford, New York, Pergamon Press, 124.
49. WEIDMAN, S. J., *in* Symposio Internazionale di Elettrofisiologia del Cuore, Oxford, Pergamon Press, 1964, in press.
50. KAO, C. Y., and GRUNDFEST, H., Postsynaptic electrogenesis in septate giant axons. I. Earthworm median giant axon, *J. Neurophysiol.*, 1957, **20,** 553.
51. WEIDMAN, S., The electrical constants of Purkinje fibres, *J. Physiol.*, 1952, **118,** 348.
52. BARR, L., and BERGER, W., The role of current flow in the propagation of cardiac muscle action potentials, *Pflügers Arch.*, 1964, **279,** 192.

FIGURE 31 An electron micrograph of the submandibular gland of the rat, depicting the apposition of the apical ends of two acinar cells. Illustrated is the terminal bar complex including desmosomes and a long length of nexus (arrow). The cytoplasm subjacent to both the nexus and desmosome appears dense. In the latter case the density is composed primarily of fibrils. OsO_4-fixed, Vestopal-embedded; section stained with uranyl acetate. × 110,000.

FIGURE 32 The apical region of two acinar cells from the same section as illustrated in Fig. 31. This electron micrograph illustrates a region similar to that shown in Fig. 31 except that the order of the desmosomes and nexus (arrow) is reversed. In either case both would form the terminal bar. × 110,000.

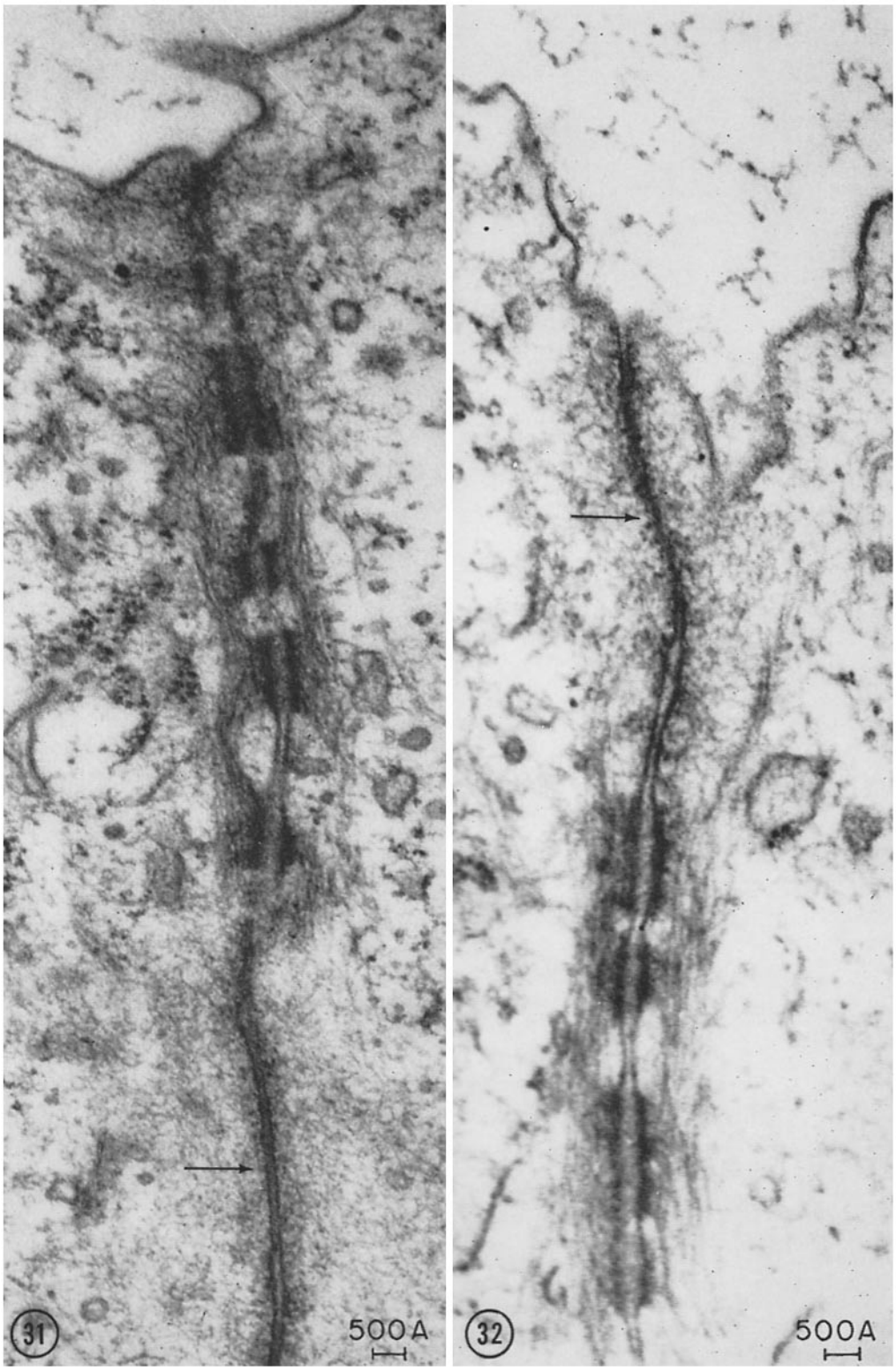
31
500A
32
500A

53. FRANKENHAEUSER, B., and HODGKIN, A. L., The after-effects of impulses in the giant nerve fibres of *Loligo*, *J. Physiol.*, 1956, **131**, 341.
54. HAGIWARA, S., and TASAKI, I., A study on the mechanism on impulse transmission across the giant synapse of the squid, *J. Physiol.*, 1958, **143**, 114.
55. VILLEGAS, R., VILLEGAS, L., GIMÉNEZ, M., and VILLEGAS, G., Schwann cell and axon electrical potential differences. Squid nerve structure and excitable membrane location, *J. Gen. Physiol.*, 1963, **46**, 1047.
56. BARR, L., BERGER, W., and DEWEY, M. M., The effects of osmolarity on propagation, longitudinal resistance and the structure of the nexus in frog atrium, *Physiologist*, 1964, **7**, 87.
57. KANNO, Y., and LOEWENSTEIN, W. R., Intercellular diffusion, *Science*, 1964, **143** 959.

FIGURE 33 An electron micrograph of three cells of an intercalated duct of rat submandibular gland. The nexus runs a considerable distance before the desmosome appears. Compare the increased cytoplasmic density along the nexus and desmosome with that in Figs. 31 and 32 of acinar cells. These two regions constitute the terminal bar. OsO_4-fixed, Vestopal-embedded; section stained with uranyl acetate. × 75,000.

FIGURE 34 An enlargement of the region encircled in Fig. 33. The adjacent plasma membranes separate for short stretches. Note that the triple-layered structure of the membrane can be discerned at these separated regions even in an OsO_4-fixed specimen, unlike the situtation in cardiac muscle. × 260,000.

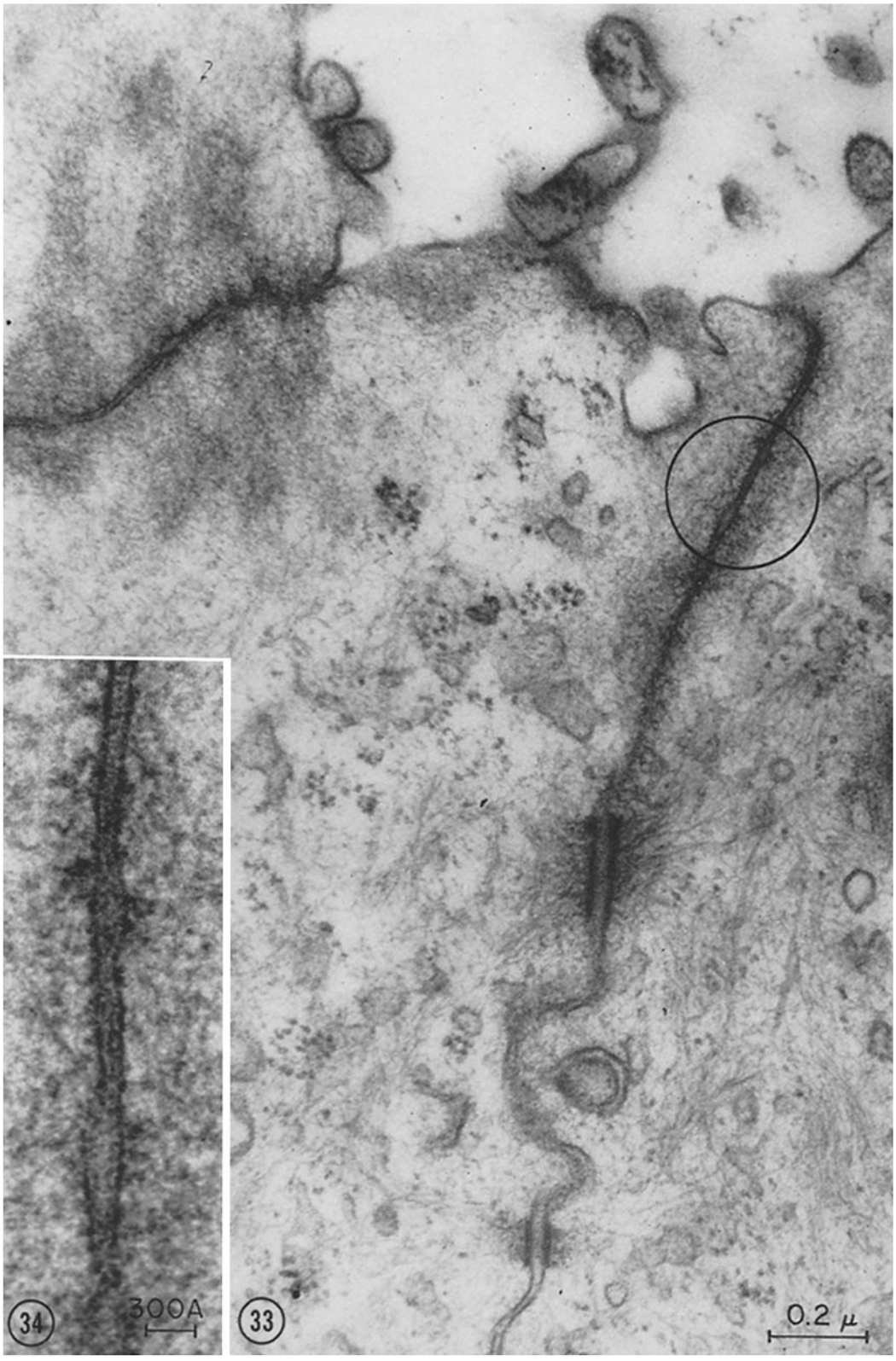
34
300A
33
0.2 μ

FIGURE 35 This section cuts obliquely through the apical borders of three epithelial cells lining the intercalated duct of rat submandibular gland. Such a section argues for the region of nexus extending continuously along the apical ends of adjacent cells. OsO_4-fixed, Vestopal-embedded; section stained with uranyl acetate. × 62,000.

FIGURE 36 An enlargement of the region encircled in Fig. 35. The adjacent plasma membranes fuse to form a nexus. × 250,000.

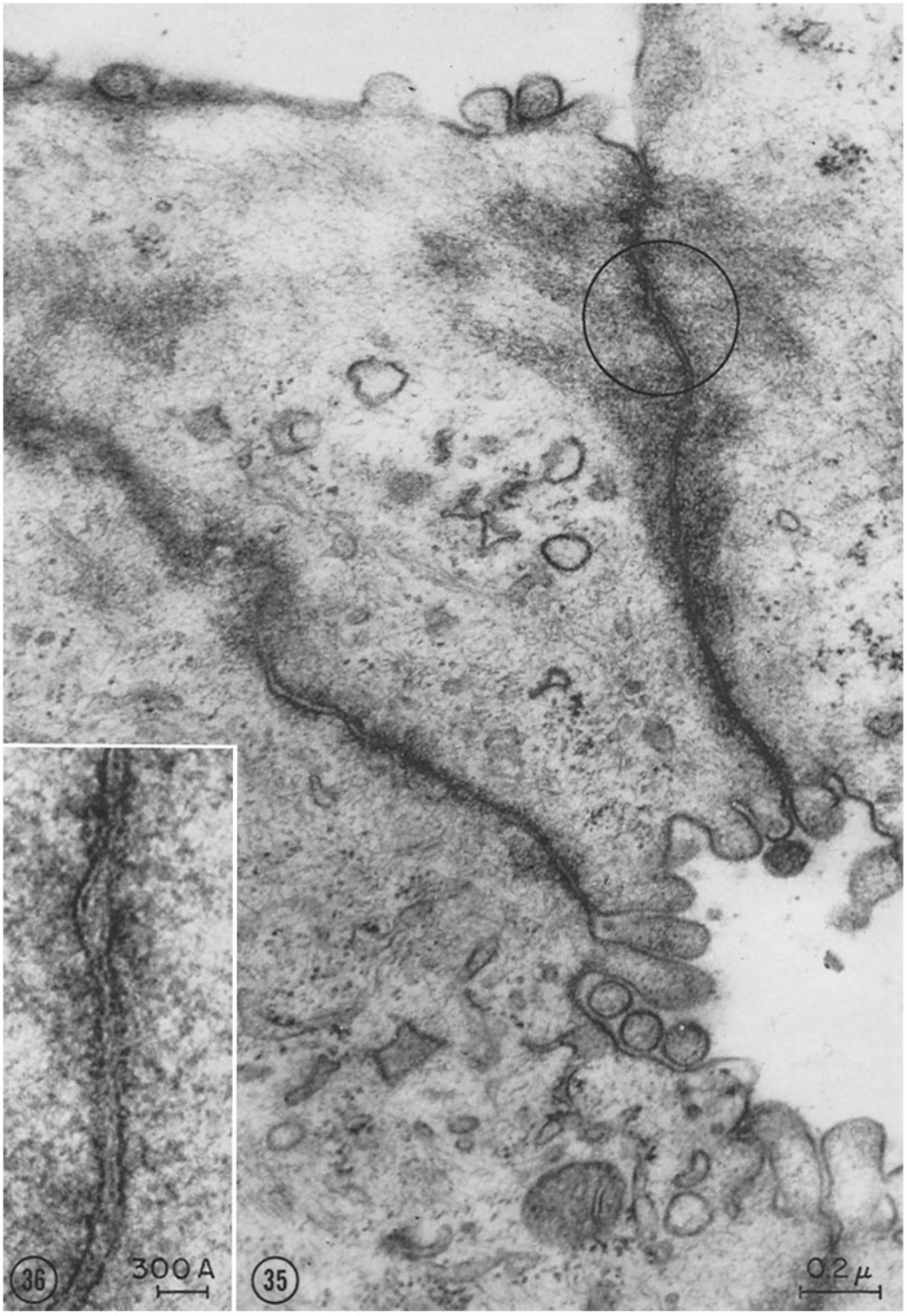
36
300 A
35
0.2 μ